JOURNAL OF GEOPHYSICAL RESEARCH, VOL. 102, NO. B6, PAGES 12,035-12,059, JUNE 10, 1997

The Chile ridge: A tectonic framework

S. F. Tebbens,[1] S. C. Cande,[2] L. Kovacs,[3] J. C. Parra,[4,5]
J. L. LaBrecque,[6] and H. Vergara[7]

Abstract. A new Chile ridge tectonic framework is developed based on satellite altimetry data, shipboard geophysical data and, primarily, 38,500 km of magnetic data gathered on a joint U.S.-Chilean aeromagnetic survey. Eighteen active transforms with fossil fracture zones (FZs), including two complex systems (the Chile FZ and Valdivia FZ systems), have been mapped between the northern end of the Antarctic-Nazca plate boundary (Chile ridge) at 35°S and the Chile margin triple junction at 47°S. Chile ridge spreading rates from 23 Ma to Present have been determined and show slowdowns in spreading rates that correspond to times of ridge-trench collisions. The Valdivia FZ system, previously mapped as two FZs with an uncharted seismically active region between them, is now recognized to be a multiple-offset FZ system composed of six FZs separated by short ridge segments 22 to 27 km long. At chron 5A (~12 Ma), the Chile ridge propagated from the Valdivia FZ system northward into the Nazca plate through crust formed 5 Myr earlier at the Pacific-Nazca ridge. Evidence for this propagation event includes the Friday and Crusoe troughs, located at discontinuities in the magnetic anomaly sequence and interpreted as pseudofaults. This propagation event led to the formation of the Friday microplate, which resulted in the transferal of crust from the Nazca plate to the Antarctic plate, and in a 500-km northward stepwise migration of the Pacific-Antarctic-Nazca triple junction. Rift propagation, microplate formation, microplate extinction, and stepwise triple junction migration are found to occur during large-scale plate motion changes and plate boundary changes in the southeast Pacific.

Introduction

The Chile ridge is a major branch of the global ridge system, extending from the junction of the Pacific, Antarctic, and Nazca plates at the Juan Fernandez microplate [*Larson et al.*, 1992, and references therein] to the triple junction of the Antarctic, Nazca, and South American plates near 46°S along the southern Chile trench [*Herron et al.*, 1981; *Cande et al.*, 1987b] (Figure 1).

The existence of a mid-ocean ridge between Rapa Nui (Easter Island) and southern South America was first predicted, on the basis of seismic evidence, by *Ewing and Heezen* [1956]. The presence of the Chile ridge was confirmed by bathymetric data collected on the Scripps Institution of Oceanography *Downwind* expedition [*Menard et al.*, 1964]. The spreading pattern on the Chile ridge was first mapped by *Herron and Hayes* [1969] and *Herron* [1971], using shipboard data, and by *Morgan et al.* [1969], using aeromagnetic data. Knowledge of magnetic anomalies and fracture zone (FZ) locations has improved due to the acquisition and analysis of additional geophysical traverses of the Chile ridge [*Herron*, 1972; *Klitgord et al.*, 1973; *Handschumacher*, 1976; *Herron et al.*, 1981] and Chile FZ [*Anderson-Fontana et al.*, 1987]. In the immediate vicinity of the Chile margin triple junction, the charting of ridge axis segments, FZs, and magnetic isochrons was further improved by detailed shipboard surveys [*Cande and Leslie*, 1986; *Cande et al.*, 1987a].

In January 1990, a team of scientists from the U. S. Naval Research Laboratory (NRL), Lamont-Doherty Earth Observatory (LDEO), the Servicio Nacional de Geologia y Mineria, and the Servicio Hidrografico y Oceanografico do la Armada de Chile conducted an aeromagnetic survey of the Chile ridge. The aeromagnetic survey and satellite altimetry data [*Sandwell*, 1993; *Smith and Sandwell*, 1995] form the basis for an improved charting of the tectonic features of the Chile ridge and its flanks.

This paper discusses the tectonic features observed along the Chile ridge and its flanks. The most significant new feature is the Friday microplate which formed during a chron 5A (~12 Ma) plate boundary reorganization. A companion paper [*Tebbens and Cande*, this issue] presents reconstructions of the southeast Pacific since the late Oligocene, showing the evolution of the Chile ridge within the framework of the southern Pacific Ocean.

Data

Tectonic interpretations are presented based on all available topographic, magnetic, and satellite altimetry data in the survey region, including the 1990 aeromagnetic survey of the Chile ridge. Bathymetry and magnetic data from a 1988 RRS *Charles Darwin* survey are presented, including four ridge-

[1]Department of Marine Science, University of South Florida, St. Petersburg, Florida.
[2]Scripps Institution of Oceanography, La Jolla, California.
[3]Naval Research Laboratory, Washington, D. C.
[4]Servicio Nacional de Geologia y Mineria, Santiago, Chile.
[5]Now at GEODATOS, Santiago, Chile.
[6]Lamont-Doherty Earth Observatory of Columbia University, Palisades, New York.
[7]Servicio Hidrografico y Oceanografico do la Armada, Valparaiso, Chile.

Paper number 96JB02581.
0148-0227/97/96JB-02581$09.00

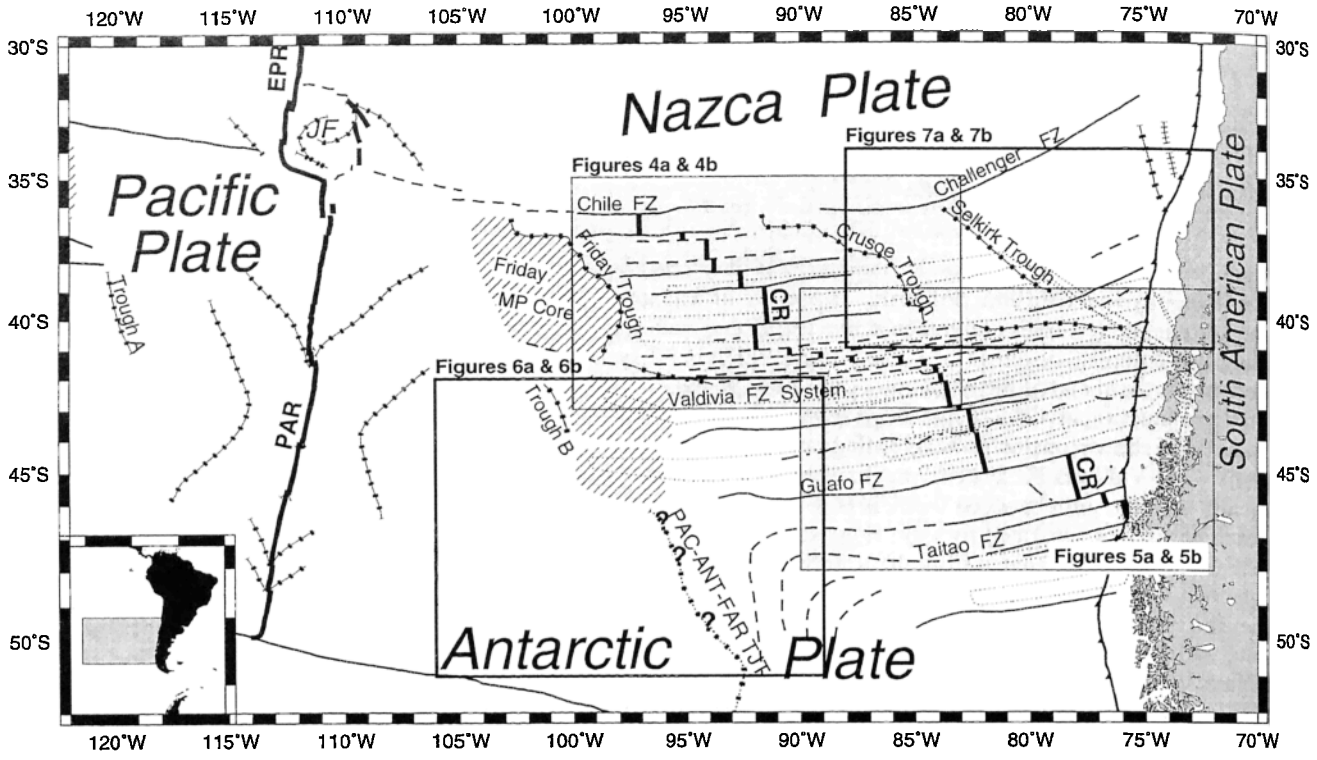

Figure 1. Major tectonic features of the South Pacific including ridge axes (heavy solid lines), FZs (solid and dashed lines are known and inferred locations, respectively), nontransform offset traces (dash-dotted lines), fossil ridge axes (railroad track pattern), transferred lithosphere (striped areas), PAC-ANT-FAR triple junction trace (TJT) (dotted lines with heavy dots), and other tectonic discontinuities (heavy lines with dots). The 1990 aeromagnetic survey lines are shown (light dotted lines). Diagonal shading denotes transferred lithosphere. Location maps for Figures 4, 5, 6, and 7 are shown.

perpendicular profiles south of the Guafo FZ. Four previously unpublished aeromagnetic lines are included which were navigated with a combination of LORAN and inertial navigation: two lines cross the Chile ridge axis, one near 38.2°S and the other near 39.5°S; and two are east-west lines located between 35°S and 36°S, to the north of the Chile ridge (D. W. Handschumacher, unpublished data, 1980).

In January 1990, a P-3 Orion aircraft equipped with a proton precession magnetometer collected a total of 37,500 km of aeromagnetic data (Figures 1 and 2). The survey lines were oriented along seafloor spreading flow lines determined prior to the survey by examining altimetry data for FZ orientations. Total intensity magnetic measurements were reduced to anomaly form by subtracting the 1985 International Geomagnetic Reference Field [International Association of Geomagnetism and Aeronomy (*IAGA*), 1987] corrected for 5 years of secular variation. The flights were almost entirely navigated with Global Positioning System (GPS). During two short flight segments when GPS was not available, OMEGA navigation was used. The OMEGA-navigated segments are the sections of the first and fourth aeromagnetic tracks north of the Guafo FZ and west of the ridge axis (181 and 355 km long, respectively) (Figure 2). Small but significant deviations (of the order of 4 km) in the linearity of the magnetic isochrons across these track segments are believed to be artifacts due to inaccuracies in the OMEGA navigation relative to the GPS navigation. In other regions with only GPS navigation, offsets of the order of 4 km are interpreted to be real.

The altitude at which aeromagnetic data are collected affects the resolution of the recorded signal. When weather permitted, lines were flown at approximately 500 m elevation, which is less than 4.0 km over the seafloor at the ridge axis. At this low altitude, the magnetic signal is comparable to a shipboard survey. A few sections were flown at altitudes as high as 3 km, due to poor weather and equipment problems, resulting in the loss of the short-wavelength information in these track segments.

Magnetic anomalies were identified by comparing them to a model based on the known sequence of geomagnetic polarity reversals [*Cande and Kent*, 1992, 1995]. Representative magnetic profiles are easily correlatable and identifiable when compared to a model profile (e.g., Figure 3). We included or, when necessary, modified the magnetic anomaly identifications and/or FZ locations of *Morgan et al.* [1969], *Herron and Hayes* [1969], *Herron* [1971], *Klitgord et al.* [1973], *Handschumacher* [1976], *Herron et al.* [1981], *LaBrecque* [1986], *Cande and Leslie* [1986], *Anderson-Fontana et al.* [1986], *Molnar et al.* [1975], and *Lonsdale* [1994].

Satellite radar altimetry data were combined with shipboard and aeromagnetic data to map the location of ridge axes and FZs. Color images were created using the gravity anomaly grid of *Smith and Sandwell* [1995] which incorporated satellite altimetry profiles from ERS 1, Geosat, and Seasat. The grid spacing is 1/20th of a degree in longitude. In this paper, "gravity field" refers to the *Smith and Sandwell* [1995] gravity grid.

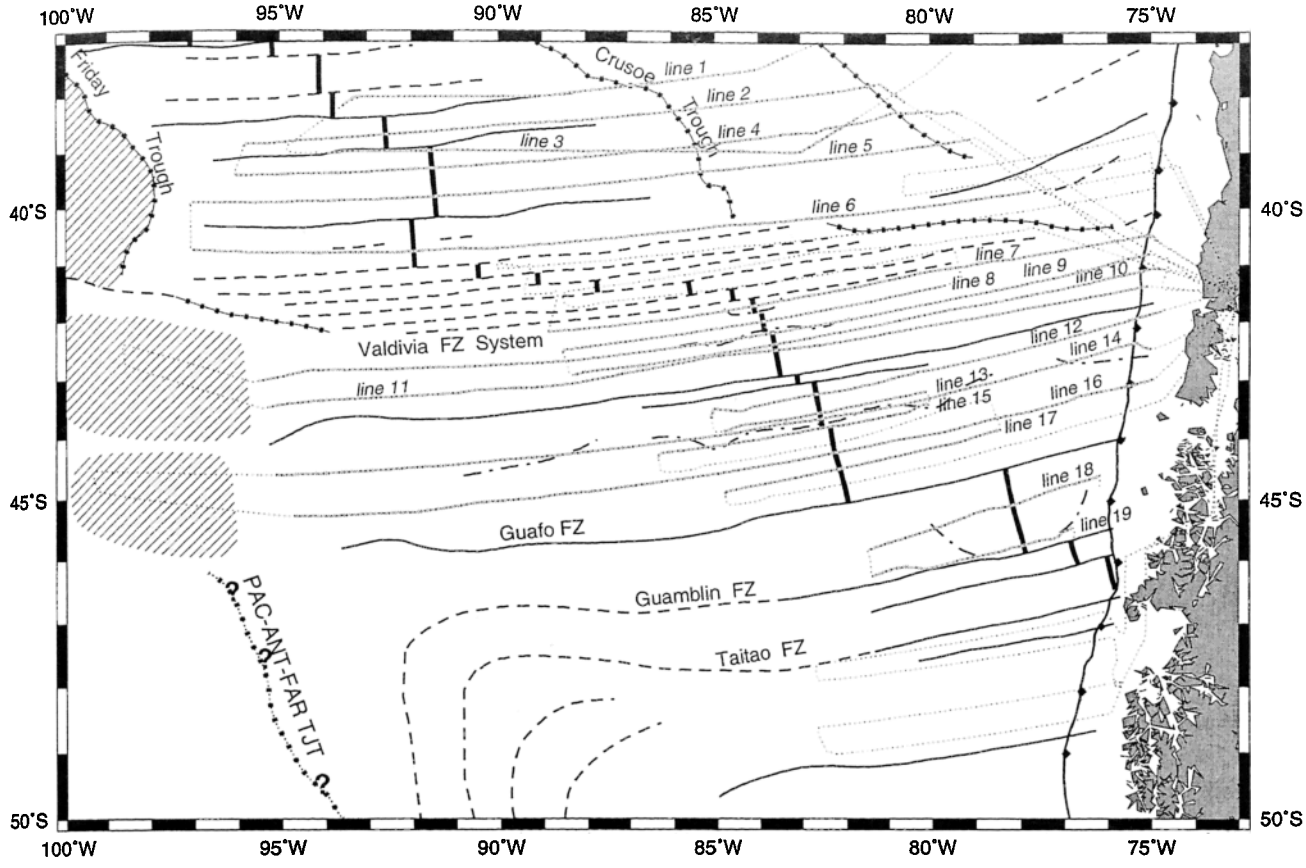

Figure 2. Location of aeromagnetic profiles shown in Figure 3. Conventions as in Figure 1.

Location of Ridge Axes and Fracture Zones from Altimetry Data

Chile ridge axis segments have previously been shown to have topographic axial rift valleys [*Herron and Hayes,* 1969; *Herron,* 1972; *Klitgord et al.,* 1973; *Herron et al.,* 1981; *Cande and Leslie,* 1986]. *Small and Sandwell* [1989] demonstrated that axial rift valleys are generally recorded as lows in satellite altimetry data. Chile ridge axis segments (located with magnetic data) are found to be associated with gravity field lows (Plate 1), which are interpreted to be axial rift valleys. In axial regions where the only geophysical data are altimetry measurements, ridge axis locations were charted along altimetry lows.

Theoretical models vary in their prediction of the location of a FZ along a geoid profile. *Sandwell* [1984] considered a simple theoretical cooling model of the oceanic crust, modeling a FZ as a step in basement with older, colder, denser crust stepping up to younger, warmer, less dense crust. The geoid mimicked that step in basement, with the FZ located at the maximum gradient of the geoid anomaly. *Parmentier and Haxby* [1986] considered thermal bending stresses which placed the FZ slightly offset from the location of the steepest gradient. *Wessel and Haxby* [1990] considered additional complexities and have a model which accounts for slip and includes flexure from a combination of thermal stresses and differential subsidence. *Wessel and Haxby's* [1990] model also places the FZ slightly offset toward the trough from the location of steepest gradient.

In this work, FZs were located using magnetic and bathymetry data, where available, and using satellite altimetry data where traditional data coverage was sparse or unavailable. The observed bathymetric expressions of FZs differ from the theoretical models. The majority of FZs observed in bathymetry profiles in this survey region are topographic troughs, as also observed at FZs formed at the fast spreading East Pacific Rise (EPR) [*Fox and Gallo,* 1989] and at the Kane FZ formed at the slow spreading Mid-Atlantic ridge [*Müller et al.,* 1990]. At the Kane FZ the mismatch between the topographic low and geoid low for 37 profiles was ~5 km, on average [*Müller et al.,* 1990]. For a FZ associated with a topographic trough the FZ location corresponds to the point at, or near, a geoid minimum [e.g., *Mayes et al.,* 1990]. Where no bathymetry data were available along the Chile ridge, a topographic trough was presumed. FZs and transforms were located at or near the geoid minimum, with the additional constraint that on both flanks of each ridge axis segment the distance between FZs was charted to be as equal as possible at conjugate distances from the axis.

Tectonic Maps and Interpretation

Detailed figures (index map, Figure 1), including the magnetic and bathymetric profiles on which the tectonic interpretation is based, were prepared for the regions north (Figures 4a and 4b) and south (Figures 5a and 5b) of the Valdivia FZ system. A similar set of figures was compiled for

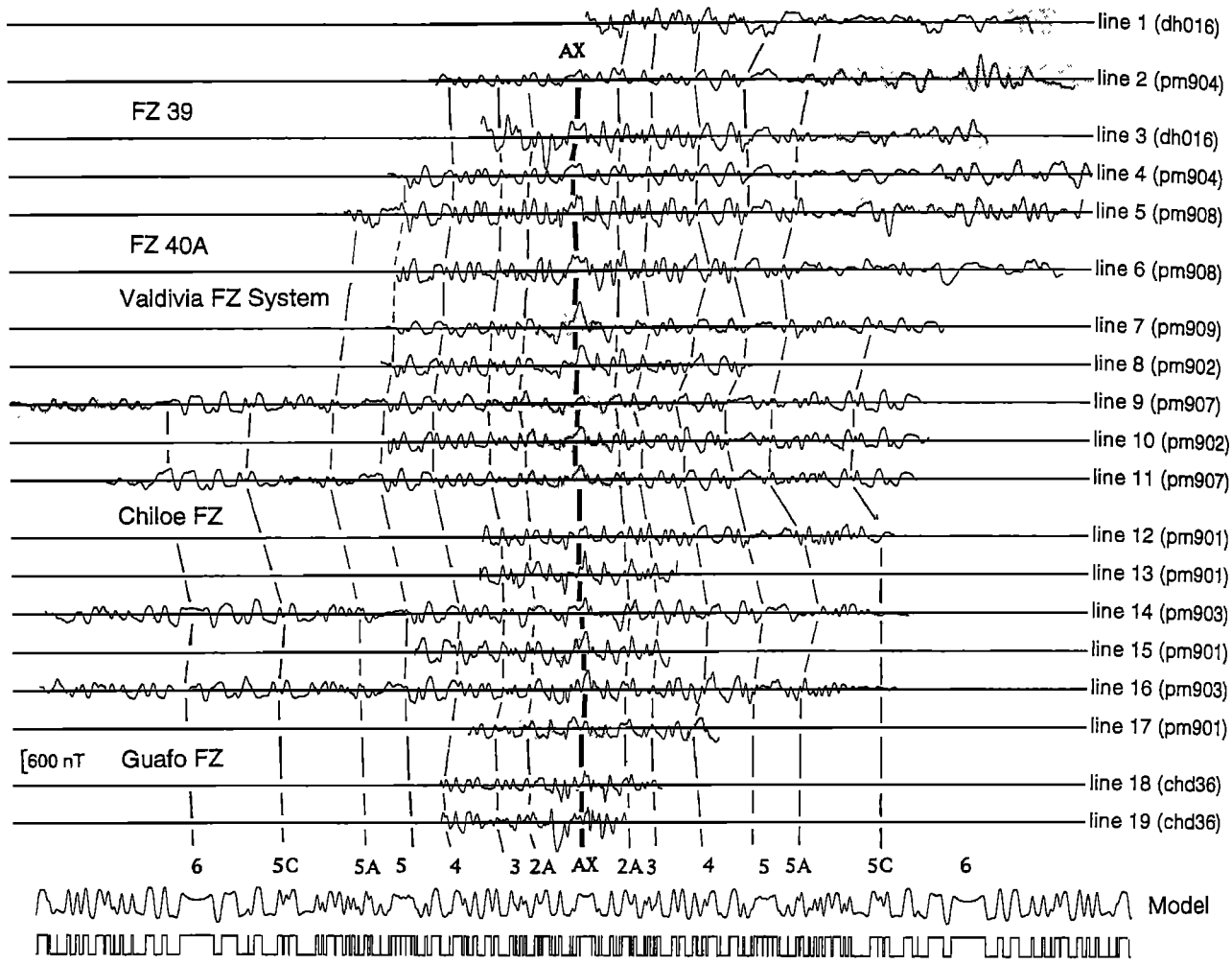

Figure 3. Magnetic profiles used in the spreading rate analysis, projected at N80°E. At bottom is a model magnetic profile created using the short interval spreading rates of Table 2. Stippling denotes data not used for the spreading rate analysis.

the regions southwest (Figures 6a and 6b) and northeast (Figures 7a and 7b) of the Chile ridge.

At present, the Chile ridge extends from the Juan Fernandez microplate to the Chile margin triple junction and is composed of 1380 km of ridge axis offset by 18 active transform faults with fossil FZs, including two complex fault systems. In addition, three nontransform offsets and their off-axis traces have been identified. The length of each ridge segment ranges from a maximum of 234 km between the Chiloe and Guafo FZs to 39 km between FZ 37 and FZ 37B to shorter lengths within the complex FZs (Table 1). The sense of shear is right-lateral along all the transform faults, except FZ 40A immediately north of the Valdivia system.

Chile Ridge North of the Valdivia FZ

The tectonic map of the northern Chile ridge region, north of the Valdivia FZ system, is based on magnetic profiles (Figures 4a), bathymetry profiles (Figure 4b) and the gravity field (Plate 1). The 1300-km-long active Chile transform fault system connects the Juan Fernandez microplate to the northernmost segment of the Chile ridge. The interpretation of the Chile transform fault and associated FZs is after *Anderson-Fontana et al.* [1986], which is based on an R/V *Endeavor* survey.

Between the Chile and Valdivia transform fault systems there are six transform faults and associated FZs. With improved data, particularly altimetry data, we find the FZ orientations in this region are ~N88°E, about 8° different from those of *Herron et al.* [1981] and *Mammerickx and Smith* [1980] (~N80°E).

FZ 37B (Figures 4a and 4b) was previously uncharted. Two gravity field lows offset by 94 km are interpreted to be ridge axis segments offset by the transform associated with FZ 37B. The location of the ridge axis segment south of FZ 37B is further constrained by a prominent central magnetic anomaly and a topographically well-defined rift valley. The location of the ridge axis segment north of FZ 37B is only constrained by a gravity field low.

Apparent tectonic complexities between FZ 37 and FZ 38 are observed in the gravity field. On the west flank there is a linear low that extends southeast from FZ 37 at 98°W to the ridge axis, just north of FZ 38B. There is a less prominent conjugate low on the east ridge flank. The trends in the altimetry data may record a pair of pseudofaults that formed by

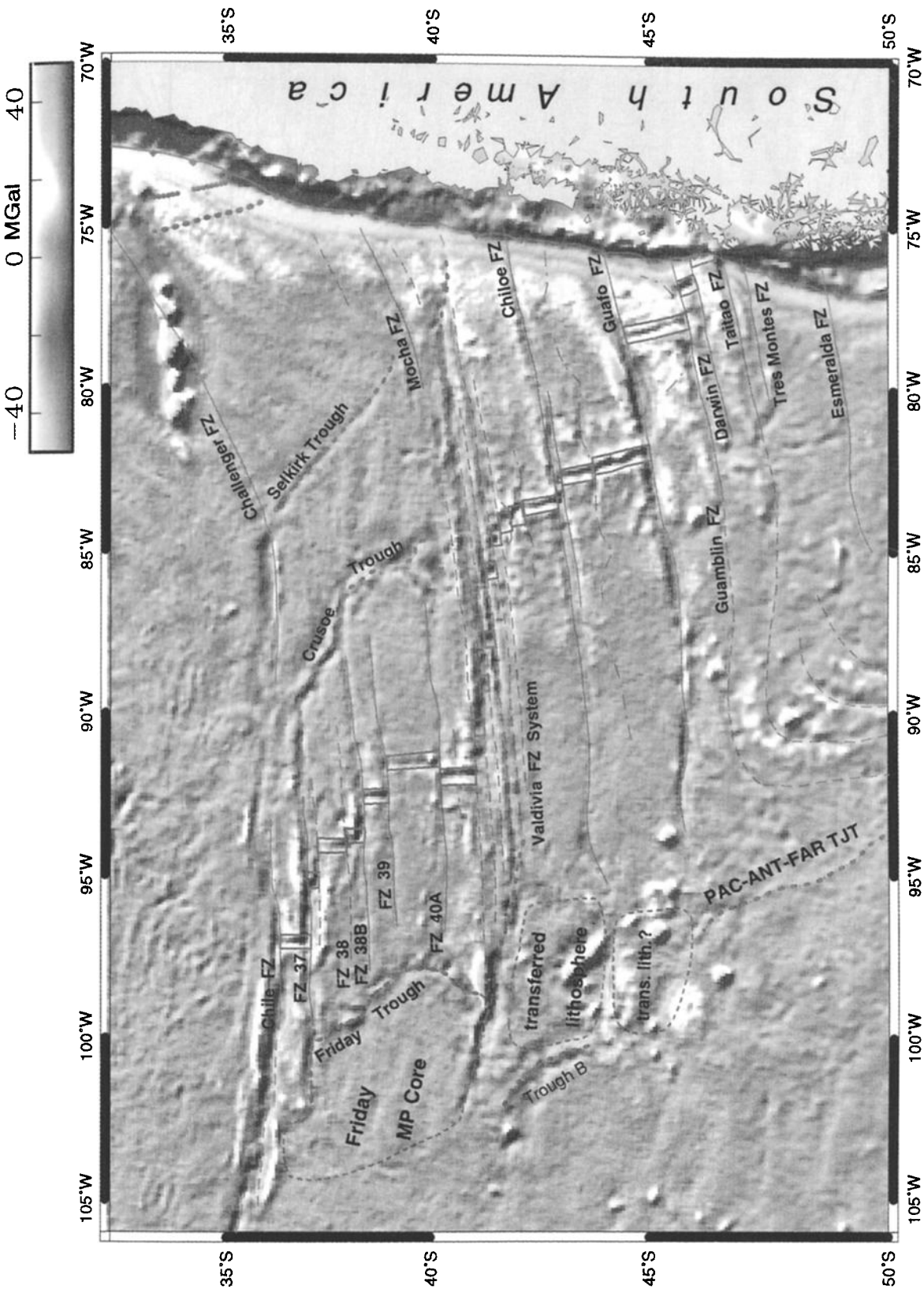

Plate 1. Tectonic interpretation of the Chile ridge and color basemap of the satellite altimetry derived gravity field of *Smith and Sandwell* [1995]. Symbols as in Figure 1. Many of the newly identified tectonic features, such as the Selkirk trough, Valdivia FZ system, Friday trough, Crusoe trough, and nontransform offset traces, are evident in the gravity field.

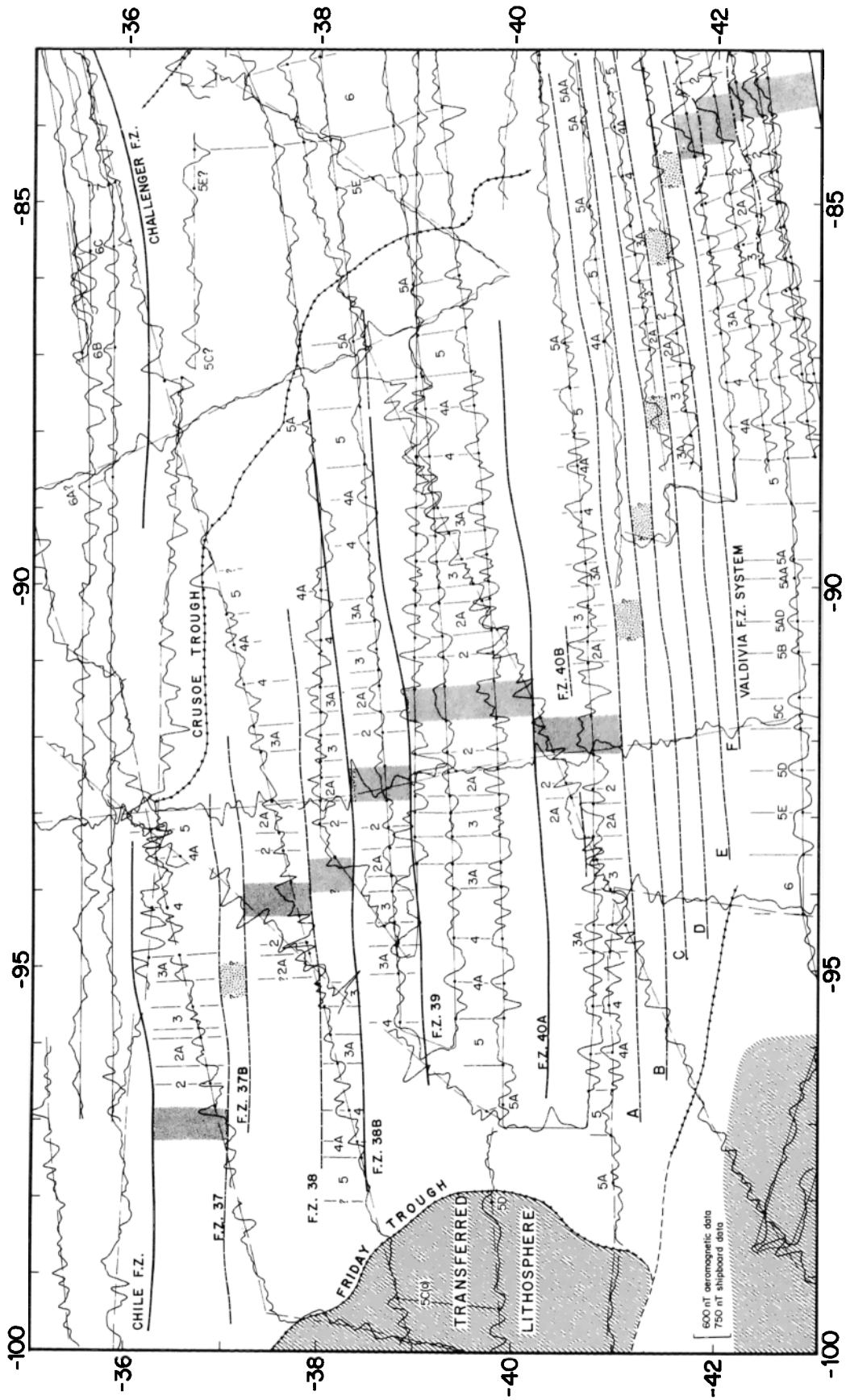

Figure 4a. Tectonic interpretation of the Chile ridge north of the Valdivia FZ system and representative magnetic data. The magnetic anomaly profiles are plotted perpendicular to the ship tracks, with positive to the north. Solid and dashed track lines are aeromagnetic and shipboard surveys, respectively. Other symbols as in Figure 1.

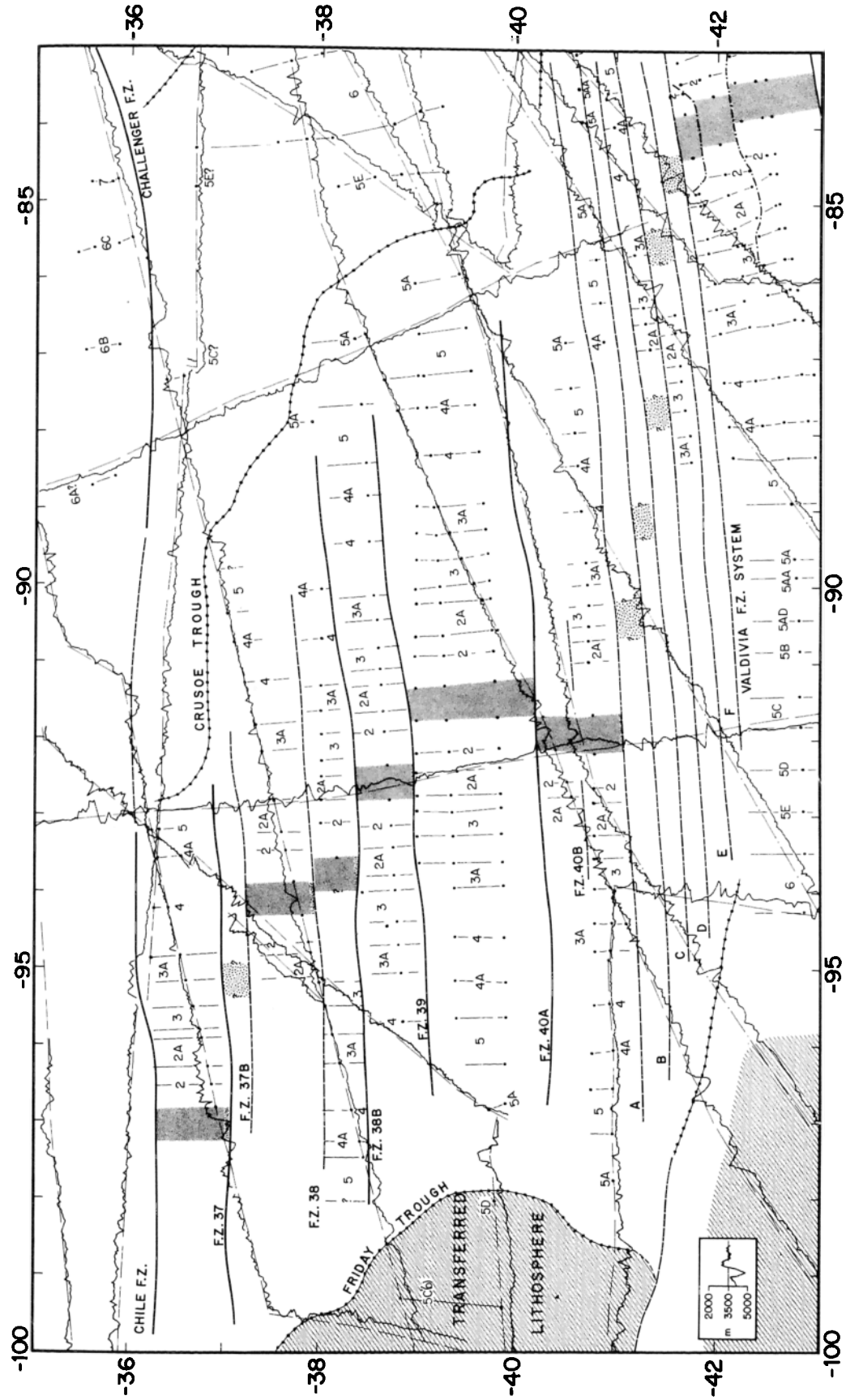

Figure 4b. Tectonic interpretation of the Chile ridge south of the Valdivia FZ system and representative bathymetry data. The bathymetric profiles are plotted perpendicular to the tracks, positive to the north. Representative satellite navigated tracks (dashed track line) and nonsatellite navigated tracks (dash-dotted track line) are shown. Magnetic interpretation from aeromagnetic surveys (Figure 4a). The track lines represent 3.5 km depth for all profiles. Other symbols as in Figure 1.

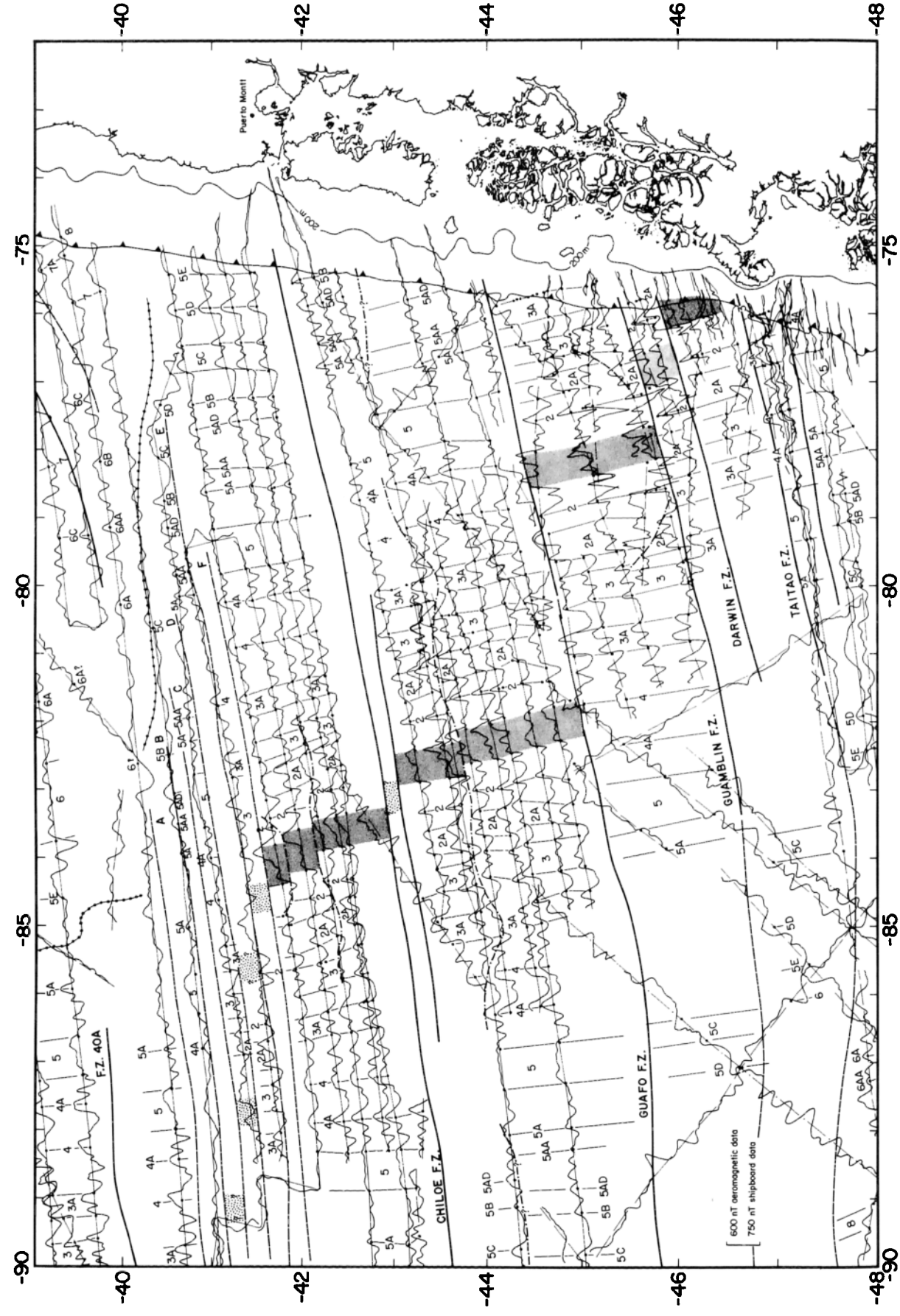

Figure 5a. Tectonic interpretation of the Chile ridge south of the Valdivia FZ system and representative magnetic data. Symbols and conventions are as in Figure 4a.

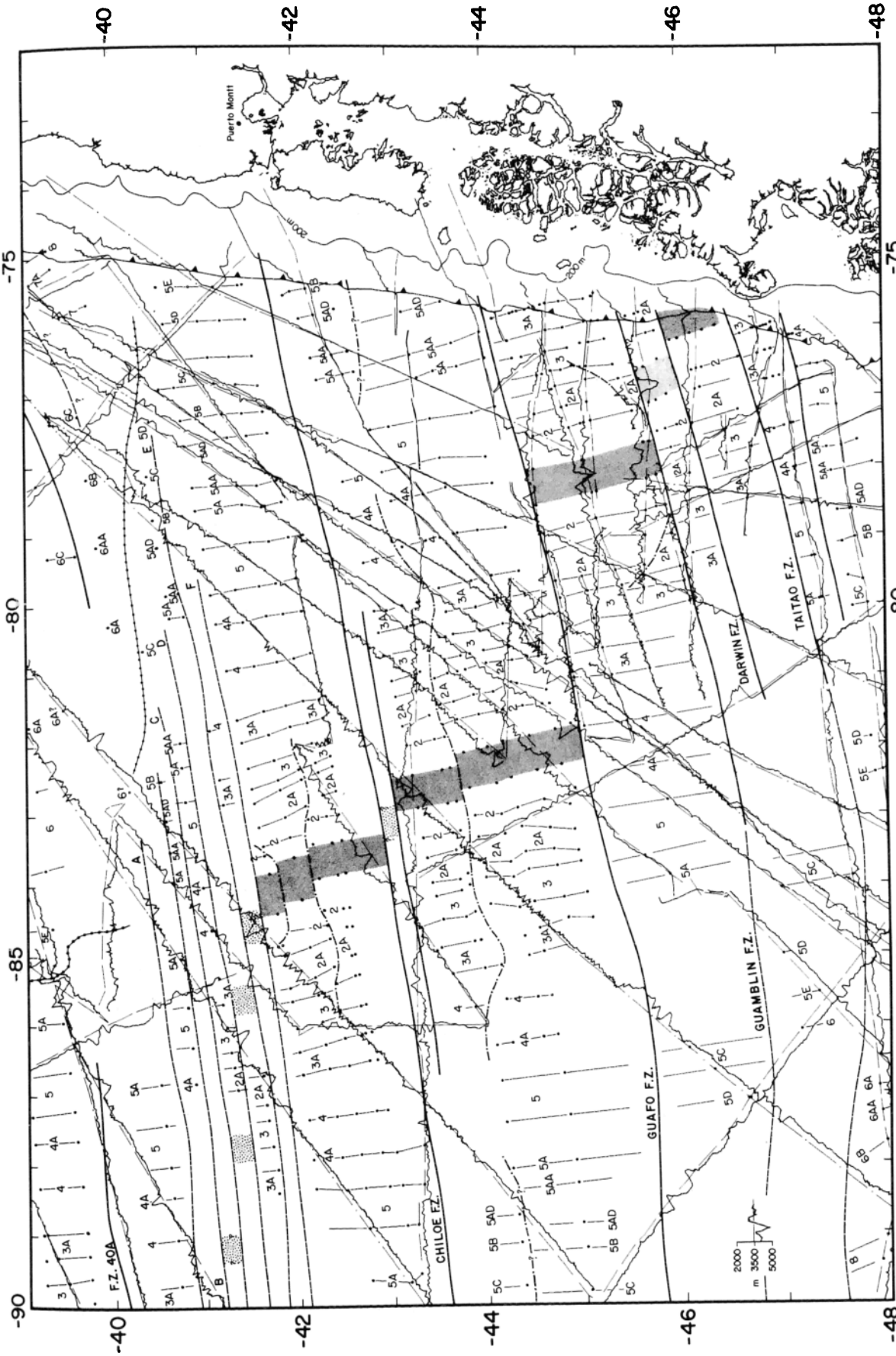

Figure 5b. Tectonic interpretation of the Chile ridge south of the Valdivia FZ system and representative bathymetry data. Symbols and conventions as in Figure 4b. The 200-m contour and subduction zone are based on shipboard bathymetry profiles and the work by *Mammerickx and Smith* [1980].

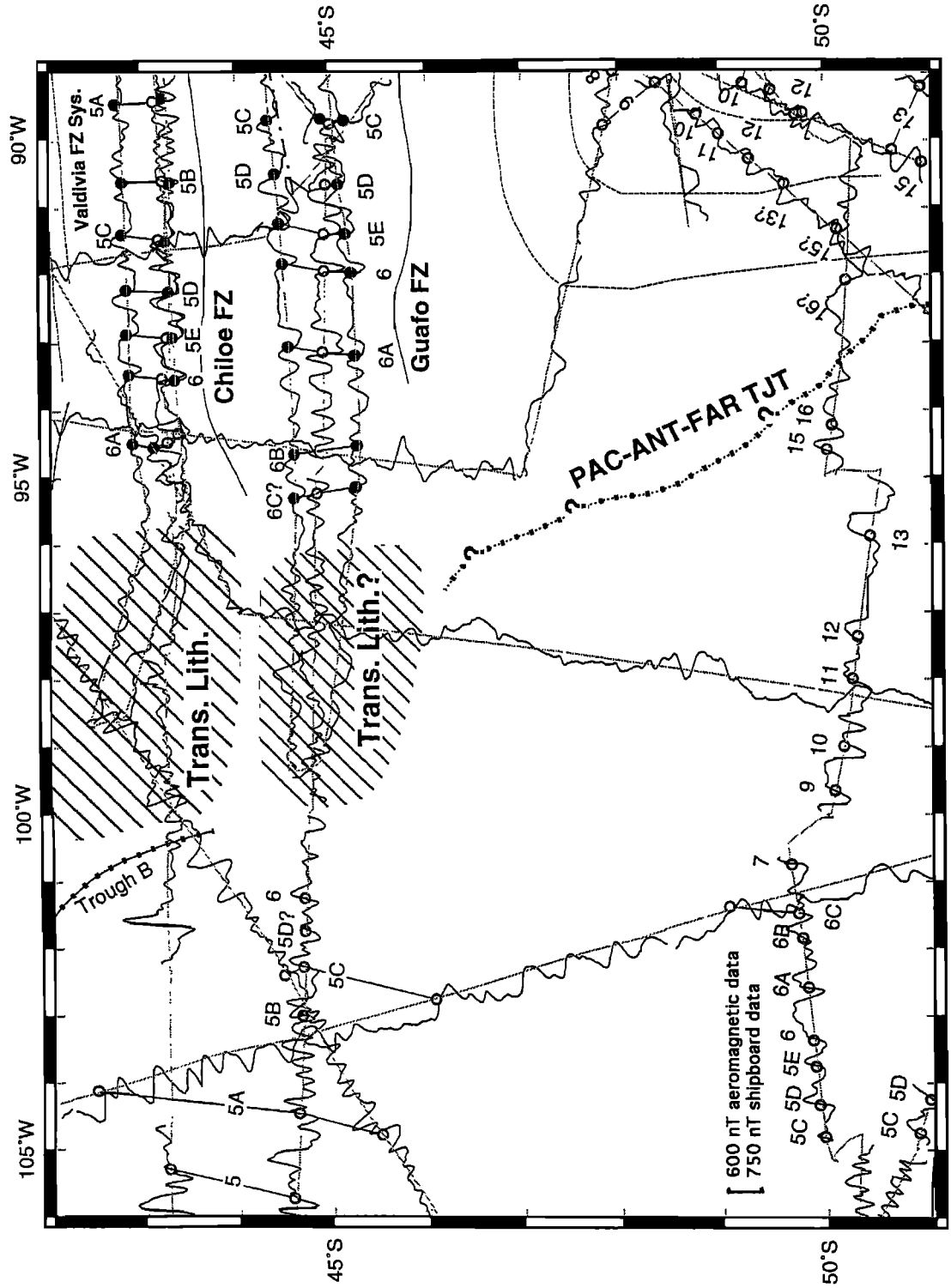

Figure 6a. Tectonic interpretation of the Antarctic plate at the boundary of the southwest flank of the Chile ridge and southeast flank of the Pacific-Antarctic ridge with all available magnetic data. Open circles denote anomaly identification from shipboard profiles (most not satellite navigated); solid circles denote anomaly identification from NRL-LDEO aeromagnetic profiles. Other symbols as in Figure 1.

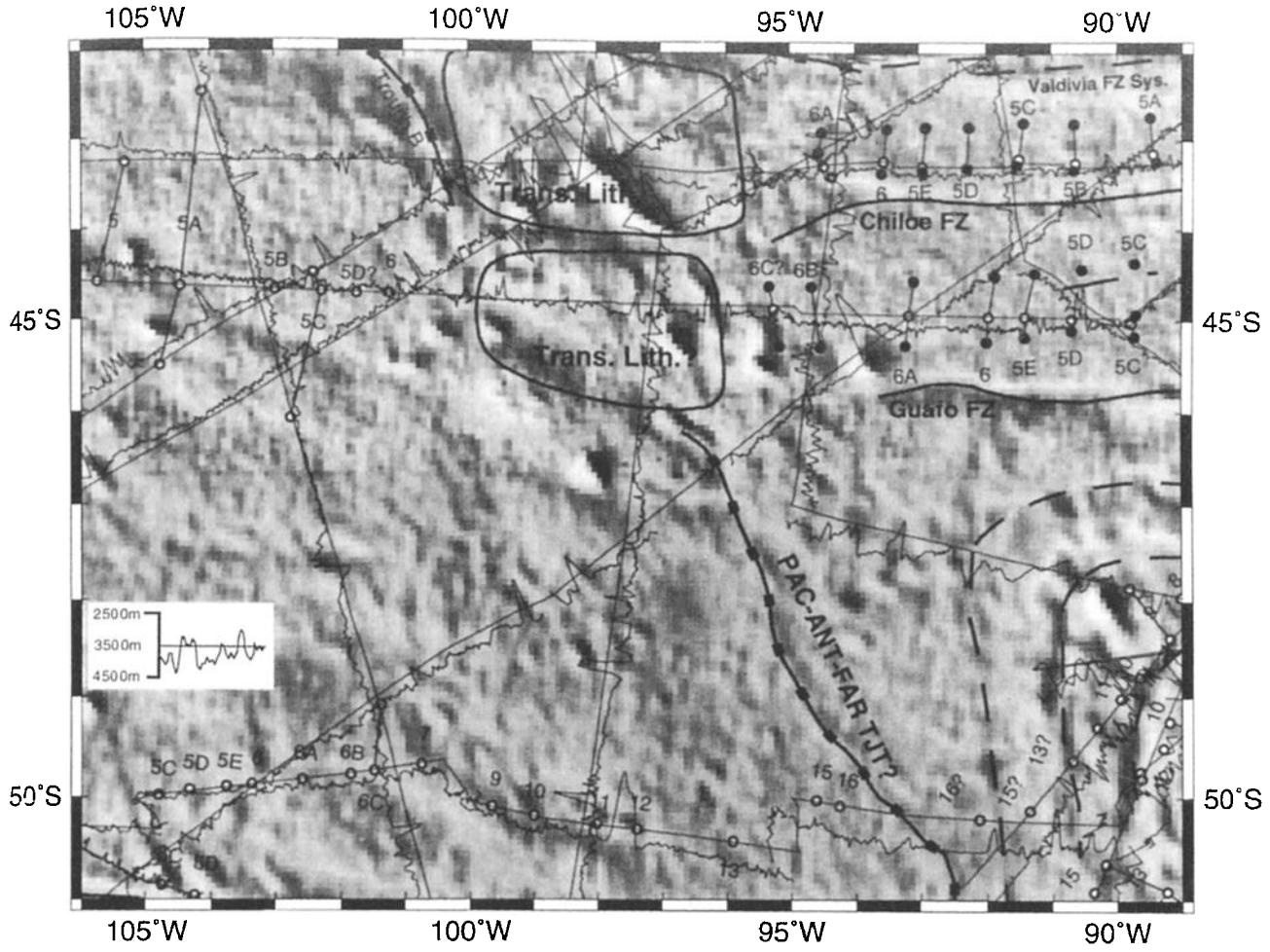

Figure 6b. Tectonic interpretation of the Antarctic plate at the boundary of the southwest flank of the Chile ridge and southeast flank of the Pacific-Antarctic ridge and all available bathymetry data. The track lines represent 3.5 km depth for the profiles. Contoured basemap is satellite derived gravity field of *Smith and Sandwell* [1995]; contour interval is 5 mGal; labeling interval of 20 mGal. Other symbols and conventions are the same as in Figure 6a.

a southward propagating ridge. The data are not definitive, and these features are not included in the tectonic interpretation.

FZ 38B, previously uncharted, offsets magnetic anomalies at the ridge axis by 102 km (Figures 4a). FZ 38B is a prominent feature in the gravity field (Plate 1) and is recorded as a bathymetric low in available bathymetry data (Figure 4b).

Between FZ 40A and the Valdivia FZ system, there is a small (~5 km), previously uncharted, off-axis isochron offset named FZ 40B. The short offset of anomalies 2A and 2 (Figure 4a) is constrained by an aeromagnetic line to the south of the offset, and a satellite-navigated cruise to the north (R/V *Thomas Washington*, 1972, cruise sot02). A topographic profile along the ridge axis shows no evidence for a FZ at this latitude, suggesting no transform now exists (Figure 4b).

Friday and Crusoe Troughs

The most prominent new features charted between the Valdivia FZ and Chile FZ are a pair of topographic troughs which bound the limits of seafloor produced by Chile ridge spreading: the Friday and Crusoe troughs. The troughs are visible as continuous lows in the gravity field (Plate 1). As will be shown in the following discussion, the propagation event which formed these troughs also transferred lithosphere from the Nazca plate to the Pacific plate, just west of the Friday trough, and formed a microplate, herein named the Friday microplate.

Magnetic data. Between the Valdivia FZ system and the Chile FZ system, the flanks of the Chile ridge record continuous magnetic anomaly sequences from the central anomaly to anomaly 5A at the Friday and Crusoe troughs (Figure 4a). Across each of these troughs we observe a discontinuity in the magnetic anomaly sequence. On the Nazca plate, where more magnetic data are available, magnetic profiles which cross the Crusoe trough (locations shown in Figure 8) are projected along flowlines and compared to model profiles (Figure 9). For the region between the central magnetic anomaly and anomaly 5A, model spreading rate profiles were created using average Chile ridge spreading rates (Table 2). To the east of the Crusoe trough, from anomalies 5D through 6B, model spreading rates were created using latitude-dependent spreading rates (Table 3). In this region the observed isochrons "fan" from north to south, with spreading rates increasing to the south (Figures 4a and 7a). Thus the use of a single (average) spreading rate for each interval for

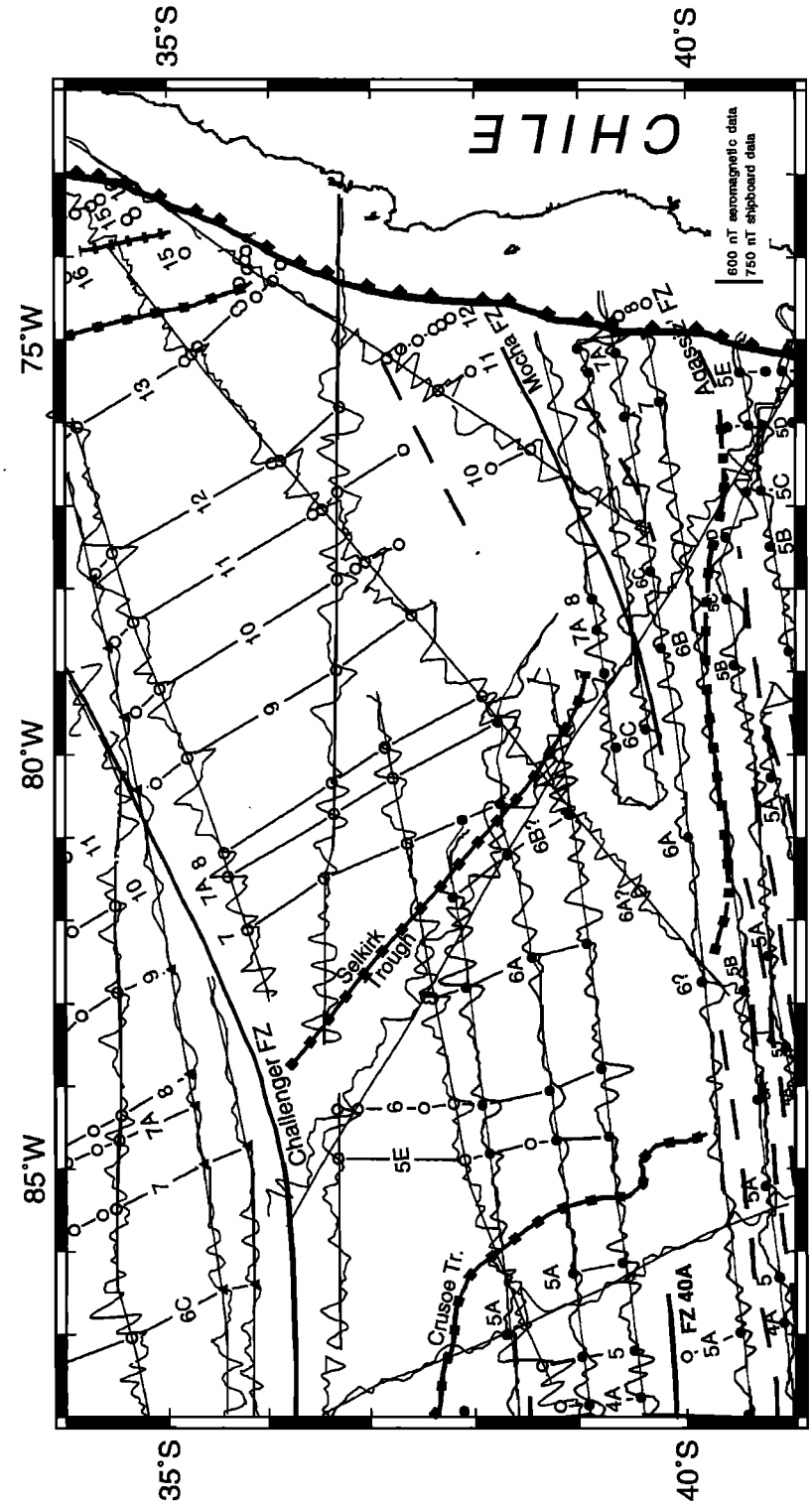

Figure 7a. Tectonic interpretation in the vicinity of the Selkirk trough and representative magnetic data. Conventions and symbols same as in Figure 6a.

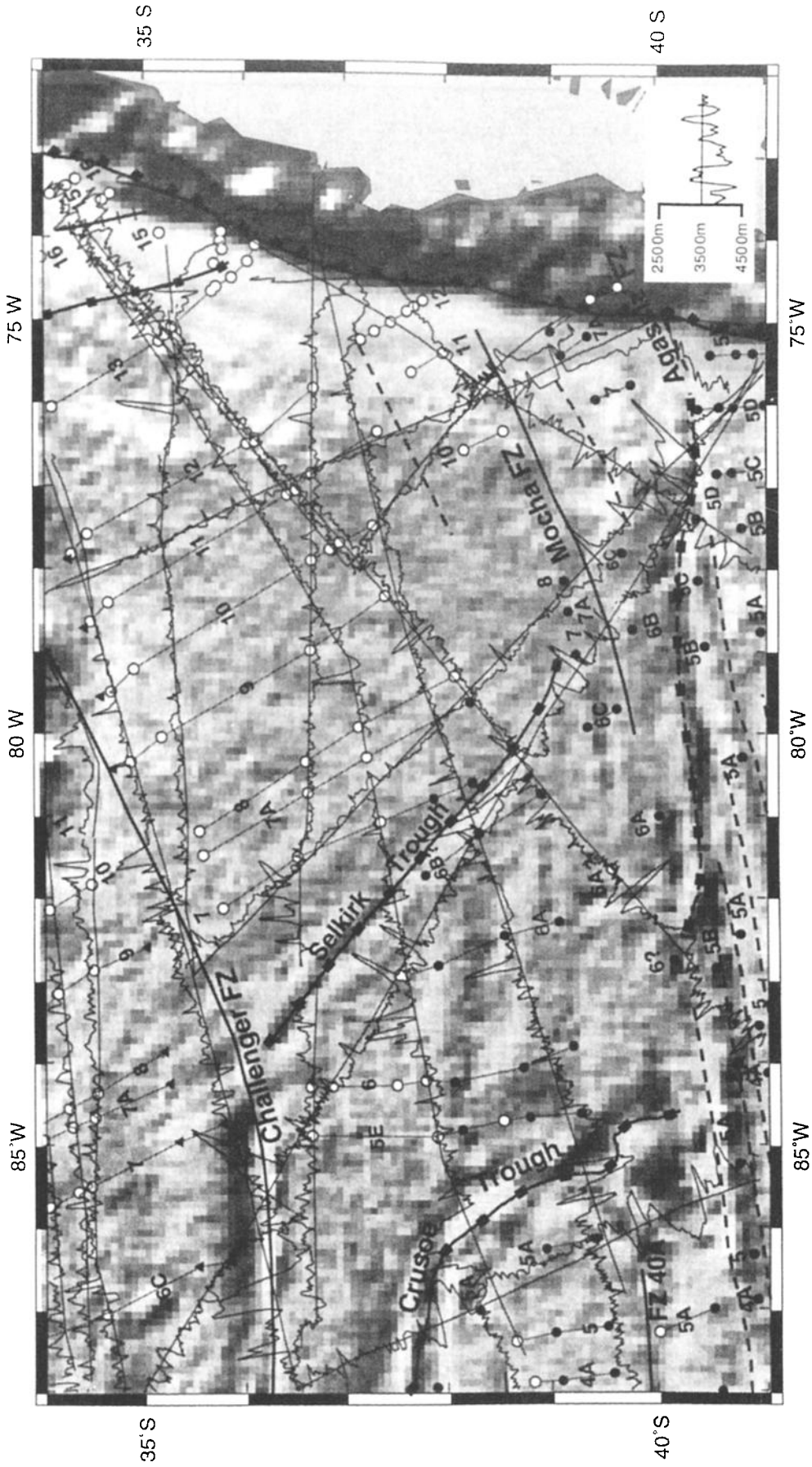

Figure 7b. Tectonic interpretation in the vicinity of the Selkirk trough and representative bathymetry data. Contoured basemap is satellite derived gravity data of *Smith and Sandwell* [1995]; contour interval is 3 mGal; labeling interval of 30 mGal. Conventions and symbols same as in Figures 1 and 6b.

Table 1. Properties of Transform Faults and Other Offsets of the Chile Ridge

Name	Latitude, +°N	Offset,* km	Offset, m.y.	Type of Offset	Distance, km	Ridge Length†, km
Chile FZ	-36.3	1124.	?	FZ		83.
FZ 37	-37.0	167.	?	FZ		31.
FZ 37B	-37.3	95.	?	FZ?		79.
FZ 38	-37.9	26.	.93	FZ		52.
FZ 38 B	-38.4	103.	3.19	FZ		66.
FZ 39	-38.9	87.	2.57	FZ		142.
FZ 40A	-40.2	-49.	1.42	FZ		96.
Valdivia system						
Valdivia A	-41.0	122.	?	FZ		27.
Valdivia B	-41.2	113.	?	FZ		24.
Valdivia C	-41.3	114.	?	FZ		24.
Valdivia D	-41.3	176.	?	FZ		25.
Valdivia E	-41.4	79.	?	FZ		22.
Valdivia F	-41.6	37.	?	FZ	28.‡	153.
41°54' offset	-41.9	12.		nontransform	37.‡	
42°12' offset	-42.2	15.		nontransform	88.§	
Chiloe FZs						
Chiloe (north)	-42.9	31.		FZ		16.
Chiloe (south)	-43.0	30.	1.75	FZ	84.§	229.
43°48' offset	43.8	15.		nontransform	145.§	
Guafo	-44.6	292.	8.46	FZ		157.
Guamblin	-45.7	82.	2.70	FZ		44.
Darwin	-45.9	53.	1.64			72.

Total ridge length is 1342 km, mean ridge length is 74.55 km, and ridge length standard deviation is 58.38 km.
* Left step is positive.
† Distance to next FZ south.
‡ Distance to next nontransform offset south
§ Distance from nontransform offset to next FZ south.

profiles at different latitudes is not appropriate. The magnetic model includes a jump in the anomaly sequence at the Crusoe trough, from anomaly 5A to 5D.

Predicted magnetic profiles for the region east of the Crusoe trough (anomalies 5D to 6A) require spreading rates faster than those determined for the Chile ridge (Figure 9). *Handschumacher* [1976] interpreted that magnetic anomalies 5E, 6, and 6A observed in this region formed at the Chile ridge. The observation of faster spreading rates is instead consistent with the interpretation that crust between the Crusoe and Selkirk troughs formed at the Pacific-Nazca ridge. This interpretation is also supported by plate reconstructions [*Tebbens and Cande*, this issue].

The magnetic anomaly sequence observed west of the Friday trough (anomaly 5D and younger) continues east of the Crusoe trough (anomaly 5E and older) (Figure 4a). This observation

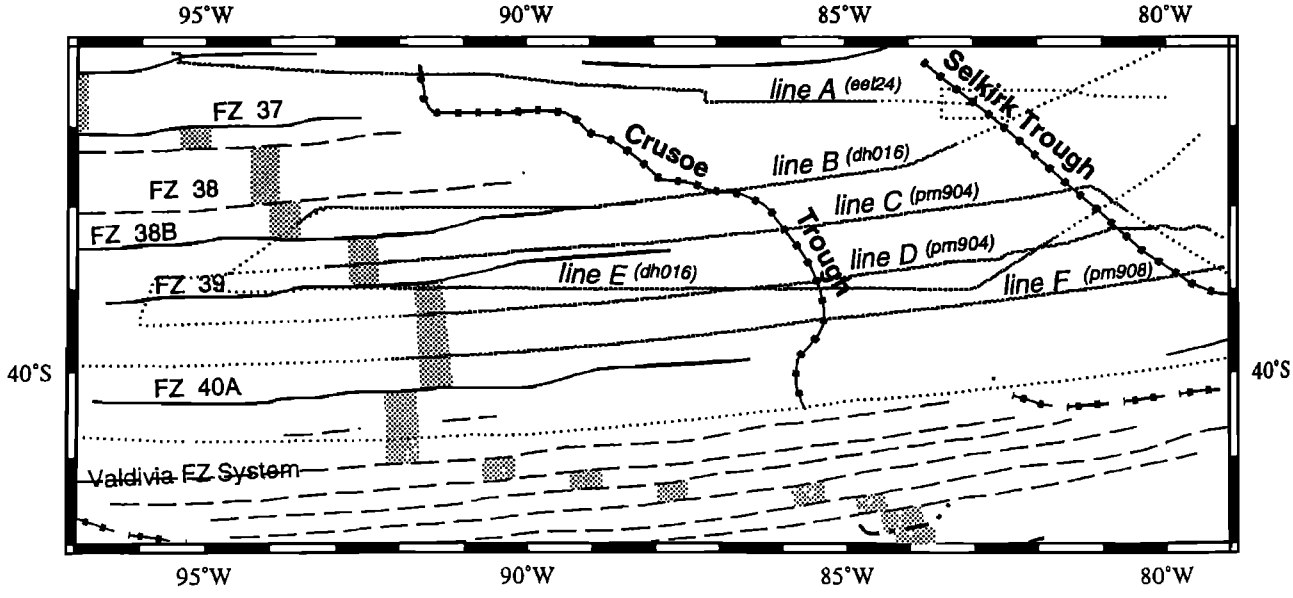

Figure 8. Location map for magnetic profiles across the Crusoe trough which are modeled in Figure 9.

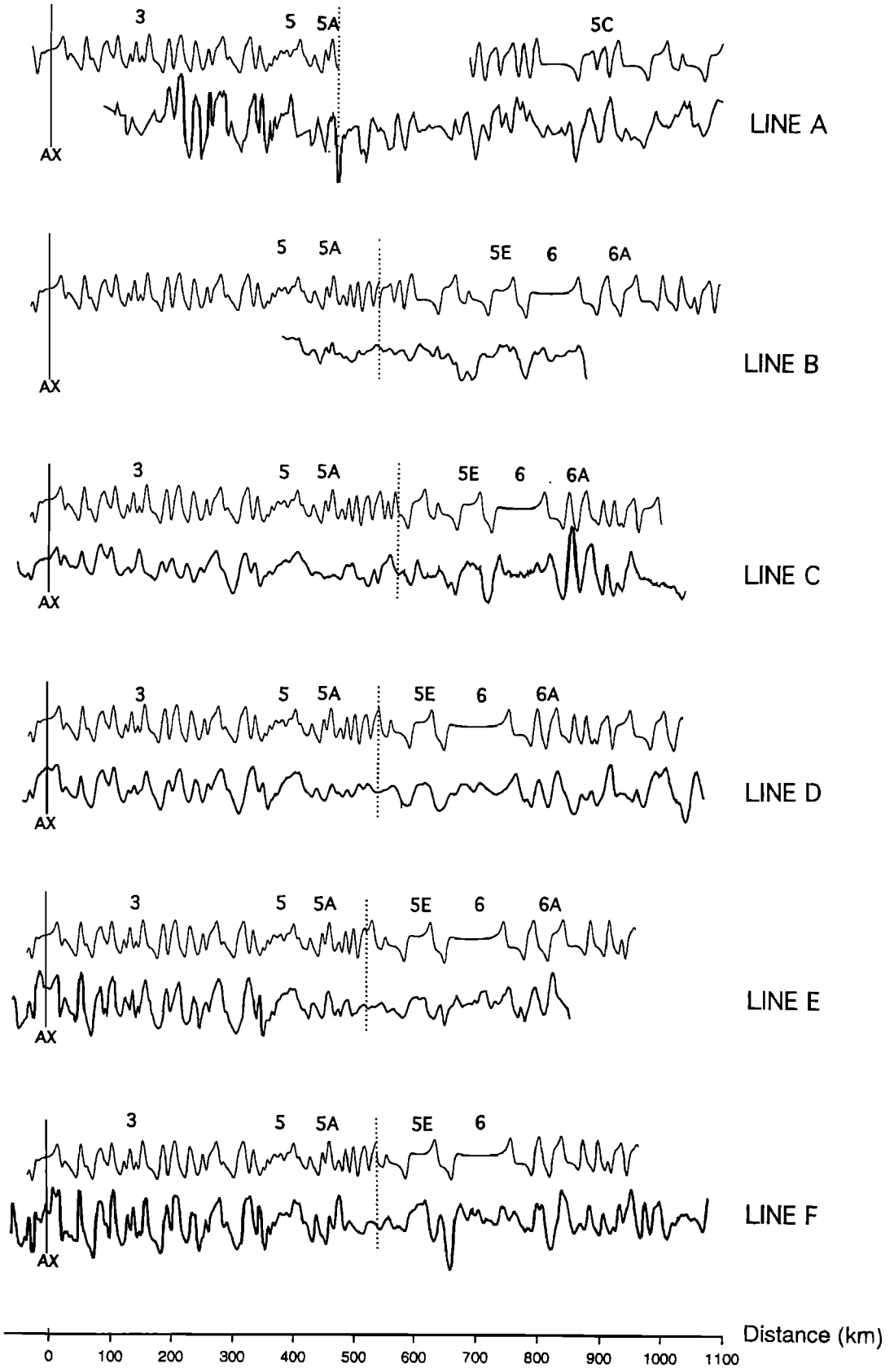

Figure 9. Observed magnetic profiles (heavy profiles) compared with model profiles created with the interpretation that there is an age discordance at the Crusoe trough, with Chile ridge spreading rates to the west of the trough and Pacific-Nazca spreading rates to the east of the trough. The locations of the ridge axis (vertical solid line at left) and Crusoe trough (vertical dotted line) are as charted on the tectonic maps.

Table 2. Neogene Spreading Rates of the Chile ridge

Time Interval (Polarity Chron)*	Time Interval, Ma	Half Spreading Rate, mm/yr	σ	*N*	Half-Spreading Rate, mm/yr
0-1n(o)	0-0.780	26.5	2.6	25	
1n(o)-2n(y)	0.780-1.770	30.3	3.0	25	
2n(y)-2An.1n(y)	1.770-2.581	32.8	4.9	26	31.3
2An.1n(y)-3n.1n(y)	2.581-4.180	29.6	3.7	27	
3n.1n(y)-3An.1n(y)	4.180-5.894	35.0	3.8	31	
3An.1n(y)-3Br.2n(y)	5.894-7.341	44.3	3.1	29	
3Br.2n(y)-4An(y)	7.341-8.699	45.0	2.9	24	45.6
4An(y)-4Ar.2n(y)	8.699-9.580	48.9	4.3	22	
4Ar.2n(y)-5An.1n(y)	9.580-11.935	40.6	3.6	16	37.8
5An.1n(y)-5Bn.1n(y)	11.935-14.800	35.5	2.8	10	
5Bn.1n(y)-5Cn.1n(y)	14.800-16.014	46.2	4.9	7	
5Cn.1n(y)-5Dn(y)	16.014-17.277	55.5	2.8	8	51.4
5Dn(y)-5En(y)	17.277-18.281	52.4	2.6	8	
5En(y)-6n(y)	18.281-19.048	61.9	1.6	4	
6n(y)-6An.1n(y)	19.048-20.518	67.4	2.5	4	61.3
6An.1n(y)-6Bn.1n(y)	20.518-22.588	57.1	7.6	2	
6Bn.1n(y)-6Cn.1n(y)	22.588-23.353	60.4	5.2	2	

*Nomenclature is after *Harland et al.* [1990], as modified by *Cande and Kent* [1992, 1995] with an appended (o) {or (y)} to specify the old {or young} age limit of each chron.

is consistent with the interpretation that a ridge (now the northern Chile ridge) propagated through and separated this once continuous sequence of anomalies. Further, the oldest magnetic anomalies observed west of the Friday trough, in a region of transferred lithosphere, become younger from south (anomaly 5D at 40°S) to north (anomaly 5C at 39°S) (Figure 4a). These observations indicate the ridge propagated through progressively younger crust from south to north.

Bathymetry data. The Friday and Crusoe troughs both consist of rough topography, often two bathymetric highs surrounding a central low (Figure 4b). Where satellite-navigated bathymetric data are available, each trough is located at the central bathymetric low. This interpretation is consistent with previous models of rifting of old oceanic lithosphere [*Mammerickx and Sandwell,* 1986], with the modification that we find no evidence for a precursor swell.

The troughs are roughly equidistant from the Chile ridge axis, with the distance between troughs decreasing from south to north (Figure 10), also suggesting northward ridge propagation. Magnetic data also indicate northward propagation: just north of the Valdivia FZ system the oldest known Chile ridge crust is anomaly 5AD(y), while just south of the Chile FZ the oldest known Chile ridge crust is younger, anomaly 5(o) (Figures 4a and 10). These magnetic data suggest propagation initiated at the Valdivia FZ system at chron 5AD(y) and ended at the Chile FZ at chron 5(o). This interpretation indicates an average propagation rate of 136 km/Myr (452 km north in 3.33 Myr). Although based on limited data, the northern Chile ridge propagation rate is remarkably similar to the initial propagation rate found for the eastern rift of the Easter microplate of ~135 km/Myr [*Naar and Hey,* 1991].

The jumps in the ages of magnetic anomalies across both the Friday and Crusoe troughs are each 5 Myr. This age jump is expected to correspond with a step in bathymetry, based on the relationship that seafloor depth increases as a function of the square root of its age [*Parsons and Sclater,* 1977]. Such topographic steps have been observed across tectonic boundaries where there are age offsets of comparable magnitude, such as FZs [e.g., *Fox and Gallo,* 1986], failed rifts [*Mammerickx and Sandwell,* 1986; *Batiza,* 1989] and propagating rifts [*Hey,* 1977]. Limited bathymetric data

Table 3. Pacific-Farallon Half Spreading rates Observed on the Nazca Plate

Anomaly Interval	Time Interval, Ma	Line A, mm/yr	Line B, mm/yr	Line C, mm/yr	Line D, mm/yr	Line E, mm/yr	Line F, mm/yr	Line G, mm/yr	Rate Used in Model (Figure 9), Where Unknown, mm/yr
5C-5D	17.31-16.03	88.84							80.
5D-5E	18.32-17.31	92.03							80.
5E-6	19.08-18.32	59.11		73.56	73.12	87.17	97.41		80.
6-6A	20.55-19.08		56.92	80.68	97.15	88.92	89.05	94.69	80.
6A-6B	22.60-20.55			46.80	52.22		62.26	97.05	80.
6B-6C	23.36-22.60				116.49			107.17	120.
6C-7	24.72-23.36							126.55	120.
7-7A	25.48-24.72	85.36						83.26	120.
7A-8	25.80-25.48	155.25							88.
8-9	27.00-25.80	87.75							79.
9-10	28.22-27.00	79.02							81.

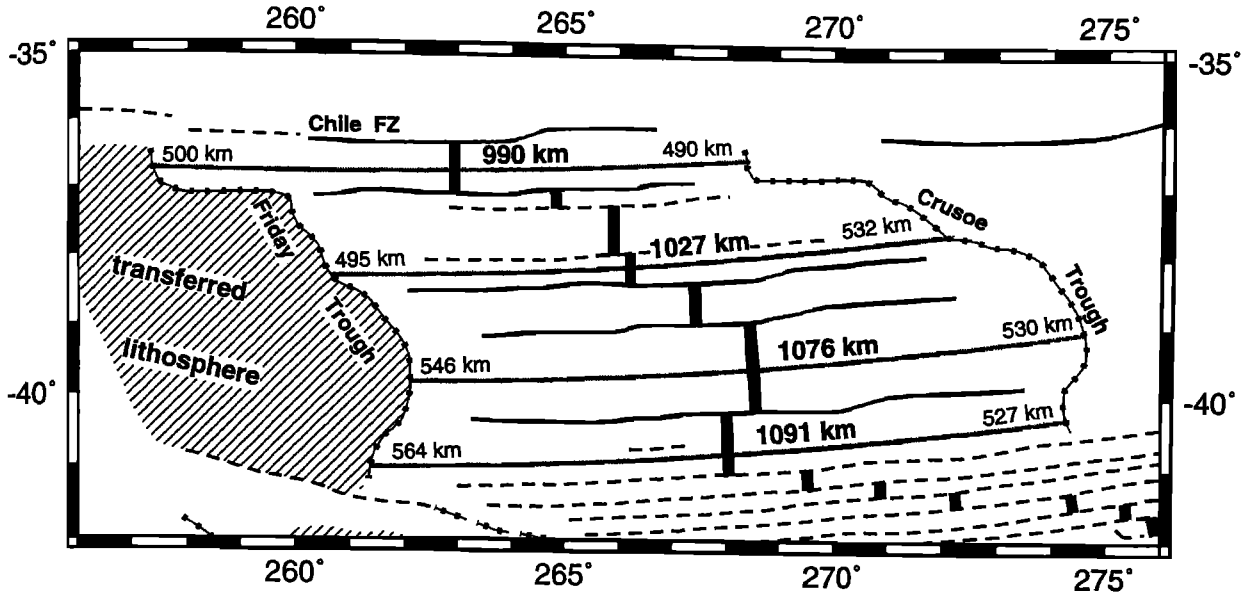

Figure 10. Observed present-day distances between the Friday and Crusoe troughs are shown in bold type to the east of the axis. Just north of the shaded lines, near each trough, are the trough to ridge axis distances. For a given segment the trough to ridge axis distances are different for each flank, suggesting asymmetrical spreading or ridge jumps. The distance between the troughs decreases from south to north, which we interpret as evidence for a northward propagation of the ridge axis through the Nazca plate. See text for further evidence. The propagating ridge axis evolved to become the northern Chile ridge.

reveal a step in the bathymetry across the Friday and Crusoe troughs (Figure 4b) in agreement with that predicted by *Parsons and Sclater's* [1977] age versus depth relationship (Figure 11). The magnitude of the Friday trough step is greater than that predicted by the model bathymetry (Figure 11), perhaps due to the proximity of the profile to Valdivia FZ A.

The shape of the Friday and Crusoe troughs are not mirror images of each other. This lack of mirror symmetry of pseudofaults is also observed at the Easter and Juan Fernandez microplates where the lack of symmetry has been explained by microplate rotation during propagation [e.g., *Schouten et al.*, 1993; *Searle et al.*, 1993]. The lack of mirror symmetry between the Friday and Crusoe troughs may be explained by their forming as pseudofaults of a clockwise-rotating Friday microplate. The lack of symmetry is the primary evidence that there was a microplate and not an instantaneous rift jump.

In summary, two prominent bathymetric troughs in the region north of the Valdivia FZ system, on the old side of anomaly 5A, bound the oldest crust formed at the Chile ridge. These troughs are interpreted to be the outer flanks of a propagating rift. The ridge began propagating shortly before chron 5A, cutting through crust formed 5 Myr earlier at the

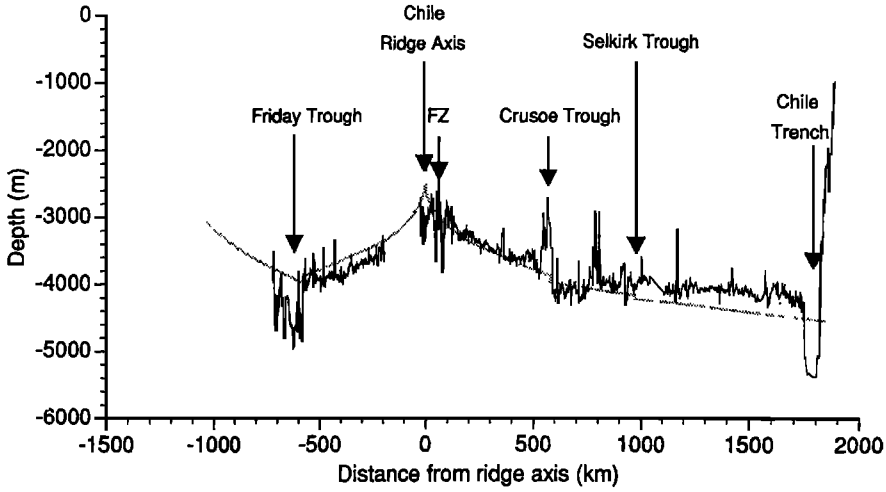

Figure 11. Observed shipboard topography across the Friday (cruise c1803) and Crusoe (cruise sot02) troughs. Model bathymetry using the formula depth = 2500 + 350*(age$^{1/2}$) (age in million years, depth in kilometers) after *Parsons and Sclater* [1977]. On both flanks, we model a gap in age from 12.6 Ma (chron 5A-middle) to 17.6 Ma (5D-old), according to the magnetic interpretation (Figure 4a). The location of the predicted gap, manifested as a step in the modeled bathymetry, corresponds with the observed location of each trough.

Pacific-Nazca ridge. The plate boundary reorganization that included this propagation formed the Friday microplate.

Valdivia FZ System

The Valdivia FZ system was previously mapped as two transforms with their associated FZs (FZ 41 and the Valdivia FZ) separated by a seismically active region with no identified ridges, transforms, or FZs [e.g., *Klitgord et al.*, 1973; *Herron et al.*, 1981; *Mayes et al.*, 1990]. This region is now interpreted to be a FZ system composed of six parallel FZs, with seismic activity in the vicinity of the ridge segments and transforms, separated by distances ranging from 22 to 27 km. FZ 41 is renamed FZ A of the Valdivia FZ system. The Valdivia FZ region is still sparsely surveyed; there are almost no magnetic data west of the ridge axis segments. The southern four ridge axis segments are well-recorded as lows in the gravity field, as are the trends of the transforms and FZs (Plate 1).

Evidence for the five narrow corridors of crust composing the Valdivia FZ system include offsets in the observed magnetic anomaly sequences (Figures 4a and 5a). Each FZ has been charted between the observed offsets in the anomaly sequences and parallel to trends observed in the gravity field (Plate 1). Bathymetric profiles crossing the Valdivia FZ system record multiple troughs, consistent with the interpretation of several FZs, but the sparse data do little to further control transform fault and FZ locations (Figures 4b and 5b).

Within the narrow corridors of the Valdivia FZ system, there are remarkably well-recorded magnetic anomalies (Figure 5a). For example, a profile between Valdivia FZs C and D on the east ridge flank records a continuous anomaly sequence from anomaly 2A (2.6 Ma) to 5AA (13.03 Ma), an interval of over 10 Myr. Surprisingly, this profile collected on the flank of a short ridge segment is indistinguishable from profiles collected on the flanks of the longer ridge segment between the Valdivia and Chiloe FZs in terms of observed spreading rate and quality of magnetic anomalies. Ridge axis locations within the Valdivia FZ system were determined by extrapolating from observed magnetic anomalies, using anomaly to ridge axis distances observed south of the Valdivia FZ system, and, for the southernmost four (of five) segments, correspond with distinct altimetry lows (Plate 1).

Bounding the Valdivia FZ system crust to the east and west are WNW trending lows in the altimetry data (Plate 1) which are interpreted as tectonic boundaries. Evidence for the eastern boundary is a change in the orientation of the magnetic anomalies and FZs across the boundary which suggests that crust to the west formed at the Chile ridge while crust to the east formed at the Pacific-Nazca ridge. There is also a jump in the age of oceanic crust across each boundary. For instance, east of the eastern extension of Valdivia FZ D there is a jump from anomaly 5C formed at the Valdivia FZ system of the Chile ridge to anomaly 6A formed at the Pacific-Nazca ridge (Figure 5a).

The oldest magnetic anomalies within the Valdivia FZ system are at least as old as anomaly 5B, as recorded on the east ridge flank between FZs C and D and FZs E and F (Figure 5a). To estimate the oldest crustal age within the Valdivia FZ system, we examined the distance, measured parallel to the Valdivia FZs, between the oldest observed anomalies within each segment of the Valdivia FZ system and the gravity lows bounding the Valdivia FZ system. Assuming that all crust within the Valdivia FZ formed at the same spreading rate as the magnetic anomalies formed farther south, between the Valdivia FZ system and the Chiloe FZ, the age of the oldest Valdivia FZ crust is ~chron 5C.

Chile Ridge South of the Valdivia FZ System: Nontransform Offsets and Their Traces

Between the Valdivia FZ system and the Chile margin triple junction, the Chile ridge is offset by four transform faults (Figures 5a and 5b). The location of the associated FZs, the Chiloe, Guafo, Guamblin, and Darwin FZs, have changed only slightly from earlier charts.

One modification is that the Chiloe FZ, from magnetic anomaly 4A (8.7 Ma) to the ridge axis, appears in bathymetric profiles to be composed of two parallel FZs 16 km apart (Figure 5b). The Chiloe FZ may be composed of two FZs in older crust as well, as suggested by some of the bathymetry profiles on the east side of the ridge axis (Figure 5b).

Along the Chile ridge, south of the Valdivia FZ system, the magnetic data are of sufficient track density to indicate the presence of several nontransform offsets with off-axis traces. Based on the assumption that nontransform offsets form at the ridge axis and thus would be symmetrical on both ridge flanks, nontransform offset traces are charted as pairs of features that are symmetrical about the ridge axis.

In the vicinity of the ridge axis, the nontransform offsets are observed as lows in the gravity field. Farther from the ridge axis, in crust older than anomaly 4A (9 Ma), nontransform offset traces that are charted on the basis of magnetic data are usually not observed in the gravity field. The dependence of FZ gravity signal on spreading rate, with lower amplitudes observed at faster spreading rates, has been shown by *Shaw* [1988] and may explain the lack of a signal observed off-axis, in crust formed during times of faster spreading rates.

Prior to the 1990 aeromagnetic survey and the availability of Geosat and ERS 1 data, the only features identified which offset the Chile ridge were simple transform faults. The recognition of nontransform offset traces and FZ systems reveals an increasingly more complicated segmentation pattern of the Chile ridge.

Pacific-Antarctic-Nazca (Farallon) Triple Junction Trace

The Pacific-Antarctic-Farallon triple junction trace, on the Antarctic plate between ~45°30'S and 53°S, is after *Cande et al.* [1989]. At 50°S, this boundary is well-constrained, as it is between magnetic anomaly 16 formed on the west flank of the Chile ridge and magnetic anomaly 16 formed on the east flank of the Pacific-Antarctic ridge (PAR) (Figure 6a). The boundary is marked by a slight trough in the bathymetry data (Figure 6b; ~50°S, 93.5°W).

West of the westernmost Chiloe FZ and Valdivia FZ system, it appears that a trough (trough B) at 101°W, 43°S (Figures 1 and 6b), separates crust formed at the Chile ridge and crust formed at the PAR. At 43°S, the oldest identifiable isochron on the west flank of the Chile ridge is anomaly 6A (Figure 6a). The oldest known isochron on the east flank of the PAR at 43°S is anomaly 5A. Between trough B and anomaly 6A of the Chile ridge is a roughly 360-km-wide region of unidentifiable magnetic anomalies and rough topography. Plate reconstructions suggest trough B formed at chron 6(o), with a

conjugate trough A located on the west flank of the Pacific-Antarctic ridge (Figure 1). With sparse data, there are at least three possible tectonic explanations. Trough B may be (1) the pseudofault of a propagating ridge, with trough A as the conjugate pseudofault; (2) one side of a separated (nonpropagating) fault, the conjugate to which is trough A; or (3) the rough-smooth boundary [i.e., *Mammerickx*, 1992] of a rapid slowdown in spreading, perhaps due to this ridge segment being a former segment of the EPR that was "captured" by the slower spreading PAR. If the last case is correct, this region may have undergone an evolution similar to that which formed the Friday and Crusoe troughs and the Friday microplate, just to the north, where the PAC-ANT-NAZ triple junction later (chron 5A) jumped northward from the Valdivia FZ system to the Chile FZ.

Discussion

Chile Ridge Spreading Rates

Chile ridge spreading rates were determined using 18 satellite navigated magnetic profiles aligned nearly perpendicular to the ridge axis (Figure 2). The magnetic profiles were projected along synthetic tracks striking N80°E, perpendicular to the ridge axis. Only well-formed magnetic anomalies, not crossing FZs or "higher-order offsets" [*Macdonald et al.*, 1991], were used (Figure 3). Average spreading rates were calculated for 17 short (~2 Myr) intervals between chron 6C (23.3 Ma) and the Present (Table 2). Spreading rates were also calculated for five longer (~5 Myr) intervals within which the spreading rates were found to be relatively constant or, in the case of chron 3A to the Present, varied in a uniform manner (i.e., a slow decrease). All reported rates are half-spreading rates.

As the Chile ridge is near the equator of the Euler pole of rotation, at any given time there is minimal variation in spreading rate along the entire ridge axis. The predicted along-axis spreading rate variation along the Chile ridge using the chron 2A Nazca-Antarctic pole of *Tebbens and Cande* [this issue] is 0.6 mm/yr (30.3 mm/yr at the northernmost segment of the Chile ridge, 80° from the pole, and 30.9 mm/yr just north of the Chile margin triple junction, 90° from the pole). Similarly, the predicted spreading rate variation of the chron 5A Nazca-Antarctic pole [*Tebbens and Cande*, this issue] was 0.8 mm/yr (37.8 mm/yr at the northernmost Chile ridge and 37 mm/yr at the Chile margin triple junction). As the modeled variations in spreading rate along-axis are slight, and far less than one standard deviation in spreading rate (σ, Table 2), the spreading rates were not adjusted for varying distance from the poles of rotation.

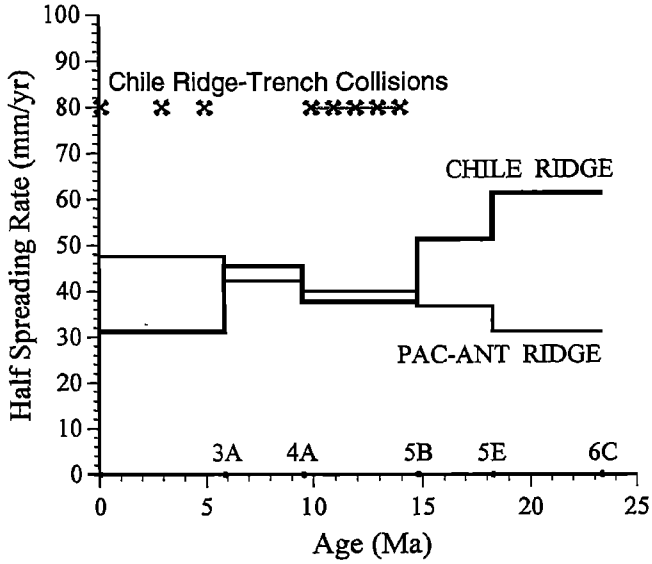

Figure 12a. Average half spreading rates of the Chile ridge for the past 25 Myr (Table 2). PAR half-spreading rates for the same time intervals were calculated by interpolating between the poles of *Cande et al.* [1995] and using these poles to determine spreading rates for a portion of the PAR adjacent to the Chile ridge, at 40°S, 112°W. There is a general decrease in spreading rate of the Chile ridge, perhaps related to the decrease in age of the subducting slab of the Nazca plate. There is a negative correlation between spreading rates of the Chile ridge and PAR. The times of two major slowdowns in Chile ridge spreading rate, 14 to 10 Ma and 6 Ma, correspond with Chile ridge/trench collisions.

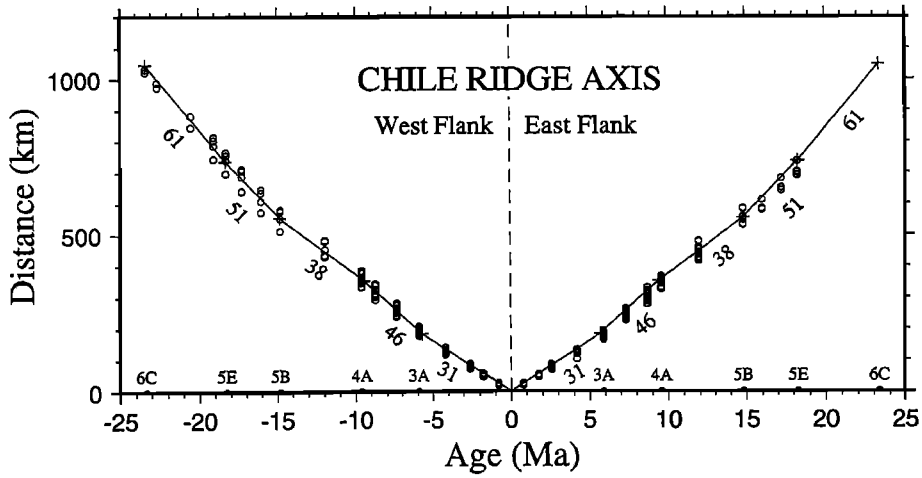

Figure 12b. Individual age versus distance from the ridge axis points (circles) determined from magnetic profiles on the east and west flanks of the Chile ridge (Figure 3). Average Chile ridge spreading rates (Table 2 and Figure 12a) are annotated, and presented graphically (solid lines), with crosses marking changes in average spreading rate. Changes in slope indicate changes in spreading rate. See text for discussion.

Our averaged spreading rates show that the Chile ridge was spreading rapidly between chrons 6C and 5E (61.3 mm/yr), was slightly slower between chrons 5E and 5B (51.4 mm/yr), slowed to intermediate rates between chrons 5B and 4A (37.8 mm/yr), increased speed between chrons 4A and 3A (45.6 mm/yr), and since then has slowed to an average of 31 mm/yr (Figure 12a). The trend toward slower spreading rates in the last few million years is supported by the observation that the current spreading rate, as measured across the central anomaly, is 26.5 mm/yr (Table 2). For variations in spreading rate on an anomaly by anomaly basis and for individual ridge segments, see *Tebbens* [1994].

Another way to analyze spreading rates is to plot age versus distance from the ridge axis [e.g., *Klitgord et al.*, 1975]. A plot of distance versus age for all reversals used in the spreading rate calculations provides an independent determination of the times of spreading rate changes (Figure 12b). In particular, changes in slope indicate times when spreading rates changed. There is minimal scatter in the observed distance from the ridge axis at each age. The observed slopes are well fit on both flanks by the calculated average spreading rates (Table 2). Spreading rates are found to be generally symmetric, although the east flank is observed to have slightly slower than average rates for the intervals from 4 to 9 Ma and 16 to 19 Ma.

Interestingly, there is a correlation between the times of decreases in spreading rates and the times of collisions of Chile ridge segments with the Chile trench. The middle Miocene slowdown between 15 and 9 Ma roughly corresponds to the time of collision of a major segment of the Chile ridge with the Chile trench between 14 and 10 Ma [*Cande and Leslie,* 1986]. The second slowdown, at anomaly 3A, is the time of the next major ridge-trench collision at 6 Ma [*Cande and Leslie,* 1986]. The most recent ridge-trench collision, 100,000 years ago, occurred during an interval of normal polarity, which was the interval of slowest observed Chile spreading rates, 0.78 Myr to Present (Table 2). Spreading rate variations within the past 0.78 m.y. are not constrained by the average values presented here, so whether this collision correlates with a distinct change in spreading rate is not resolved. Whether there is a significant causal relationship between Chile ridge spreading rates and Chile ridge-trench collisions is unclear: a corresponding increase in spreading rate during intervals of transform fault subduction is clearly observed during the 10 and 6 Ma transform subduction, but not during the transform fault subduction preceding the 3 Ma (and 0.1 Ma) ridge-trench collisions (Table 2).

The distinct decrease in Chile ridge spreading rate at 6 Ma (chron 3A) was noted by *Cande and Kent* [1992] to be nearly synchronous with other circum-Pacific events, including distinct increases in spreading rates on the Pacific-Antarctic and Southeast Indian ridges, a clockwise rotation in spreading direction on the Southeast Indian ridge [e.g., *Munschy et al.*, 1992], and the initial rifting of the Lau Basin at 5.6 Ma [*Leg 135 Scientific Party,* 1992]. These events are synchronous with a Chile ridge-trench collision, discussed above, and slightly precede the initial propagation of the east ridge of the Juan Fernandez microplate at 5.1 Ma [*Bird and Naar,* 1994].

Formation of the Valdivia FZ System

South of the Valdivia FZ, magnetic profiles (Figure 6a) and gravity field trends (Figure 6b) document a 10° counterclockwise rotation in spreading direction on the Chile ridge at anomaly 5C. Evidence for this rotation is a 10° change in azimuth of magnetic isochrons from chron 5D to chron 5B at 43°S (Figure 6a) and a change in the strike of the Chiloe and Guafo FZs (Figure 6b). The counterclockwise rotation of the Chile ridge placed the Agassiz transform under extension and led to the initiation of the Valdivia FZ system spreading within the separated Agassiz transform.

The rotation of the Chile ridge from chrons 5D to 5B also placed the other transforms of the Chile ridge, all right-lateral offsets, under extension, but only the Agassiz transform developed into a multiple offset transform system. The relative length of the Agassiz transform to other Chile ridge transforms may explain why it was the only transform to separate during the ridge rotation. The Agassiz transform was over 750 km long, more than 3 times longer than any other Chile ridge transform. The Agassiz transform connected the (then) northernmost Chile ridge to the PAC-ANT-NAZ triple junction [*Tebbens and Cande,* this issue], analogous to the present-day Chile transform.

Friday Microplate

At chron 5A(o), the Chile ridge propagated northward from the Valdivia FZ toward the Challenger FZ through then 5-Myr-old crust (approximately anomaly 5D) formed at the Pacific-Nazca ridge. The scars of this propagation event are the Crusoe and Friday troughs, the limits of the oldest crust formed along this section of the Chile ridge. As a consequence of this propagation event, crust was transferred from the Nazca plate to the Antarctic plate which comprises the Friday microplate core (Figures 1 and 13).

Figure 13 presents a schematic representation of the plate boundaries just before and after the chron 5A propagation event and demonstrates the propagation-induced reorganization of plate boundaries (upper) and the plate boundary origins of the crust comprising each plate. The chron 5A propagation event resulted in a major plate boundary reorganization, discussed below.

Initial propagation. The propagation event appears to have initiated from the northernmost transform fault of the newly formed Valdivia transform fault system (Figure 13, before). Intratransform origins of propagating ridges of microplates have been studied by *Bird and Naar* [1994], who found the eastern rifts of the Easter and Juan Fernandez microplates also apparently initiated along transform faults. The location of crust which later would form the core (transferred lithosphere) of the Friday microplate is indicated for reference.

During propagation. The propagating ridge separated Nazca plate crust formed at the EPR and transferred lithosphere located between the propagating ridge and the EPR from the Nazca plate to the Antarctic plate (Figure 13, after, "Friday microplate core"). The EPR was west of the initial location of the propagating ridge. The southernmost EPR became an "overlapped ridge" in microplate terminology [*Naar,* 1992] and formed the western microplate boundary. The transferred lithosphere was not rigidly attached to any of the major plates (Pacific, Antarctic, or Nazca plates). The transferred lithosphere (labeled Friday microplate core in Figures 1 and 13) and material accreted at the ridge axes compose the Friday microplate. Assuming the oceanic plates behaved rigidly, the overlapped ridge slowed and possibly changed spreading direction relative to the rest of the EPR [e.g., *Naar,* 1992]. In the gravity field, there is a slight, but distinct, linear low at

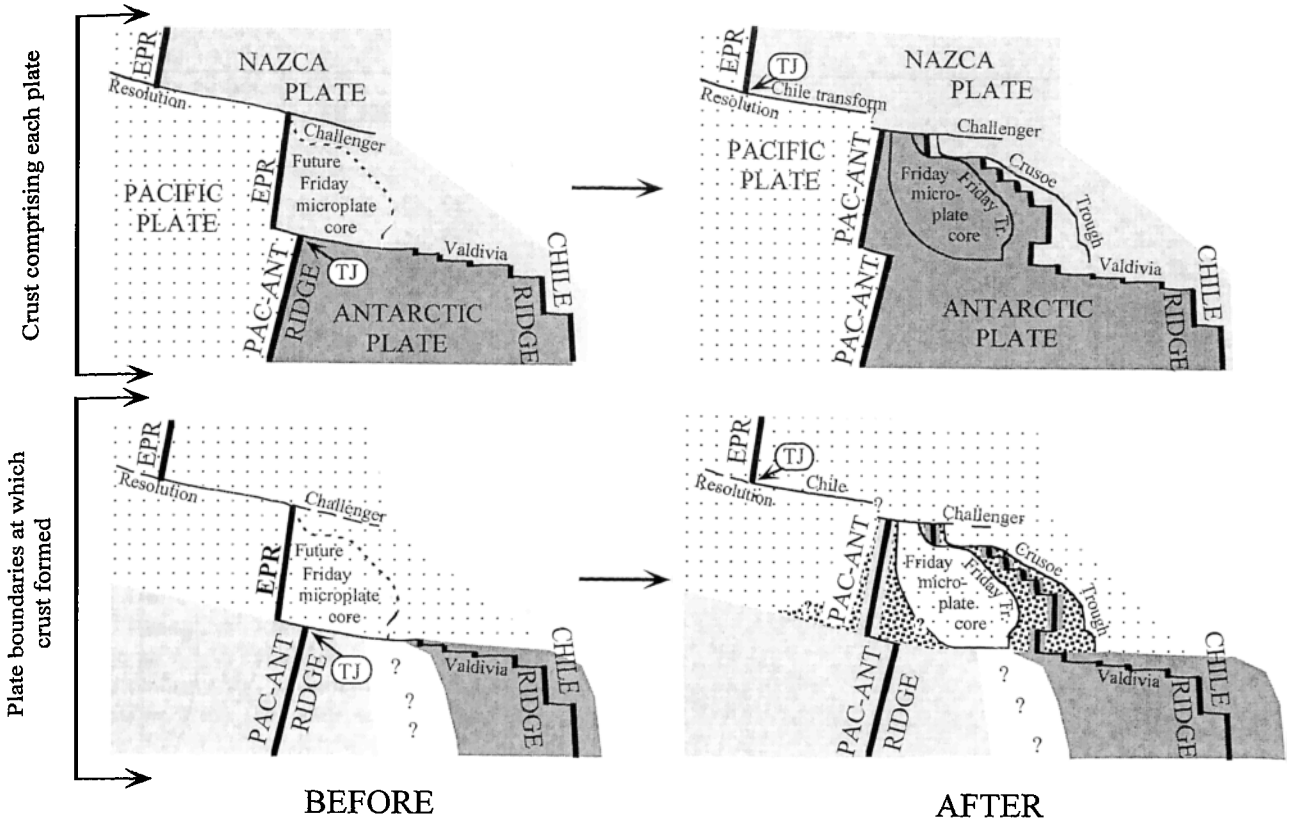

Figure 13. Schematic plate reconstruction (left) before and (right) after the chron 5A plate boundary reorganization. The top row depicts which crust comprises each plate. Note that a region north of the Valdivia transform is transferred from the NAZ plate to the ANT plate. The bottom row depicts at which plate boundary the crust formed. Note that the section of ridge south of the Challenger FZ changes from southernmost EPR to northernmost PAR due to the reorganization. Note that the northernmost Chile ridge extends 500 km north, from terminating at the Valdivia transform (before) to the Chile transform (after).

~103°W on chron ~5A crust on the east flank of the EPR, near the western boundary of the Friday microplate (Plate 1). This low trends parallel to the nearby magnetic isochrons (e.g., anomaly 5A) on the Antarctic plate and appears to reflect ridge axis adjustments. Again assuming the plates were rigid, active transform faulting occurred along the northern and southern boundaries of the microplate: the Chile transform and the former Agassiz' transform [*Tebbens and Cande*, this issue], respectively.

Propagation complete. Propagation ceased when the propagating ridge reached the Challenger FZ. The Challenger FZ formed at an offset of the Pacific-Farallon EPR. The new ridge axis apparently rapidly adjusted to accommodate the same plate motions as the Chile ridge south of the Valdivia FZ system and is now the northern Chile ridge (between the Valdivia FZ system and the Chile FZ). The Challenger FZ became a reactivated transform (the present-day Chile transform) connecting the new northern Chile ridge to the new location of the Pacific-Antarctic-Nazca triple junction. The extinct Friday microplate became incorporated into the Antarctic plate. The extinct Friday microplate includes the transferred Nazca plate crust and the crust which formed at the microplate boundaries (Figure 13, lower row). The southern boundary of the microplate, a portion of Valdivia FZ A, which had been an active transform fault during rift propagation, was abandoned. This is similar to the southern boundary of the Mathematician microplate, which is defined as an abandoned transform fault of the O'Gorman FZ [*Mammerickx et al.*, 1988]. The ridge to the west of the extinct microplate, the southernmost section of the EPR prior to propagation, became the northernmost segment of the Pacific-Antarctic ridge.

The extinct Friday microplate is now bounded to the north by a poorly located portion of a former transform (perhaps part of the Challenger FZ, Figure 13), to the south by a portion of Valdivia FZ A, to the west by chron 5A crust on the Pacific-Antarctic ridge east flank, and to the east by chron 5A crust on the Chile ridge west flank.

The chron 5A plate boundary reorganization resulted in the most recent northward migration in the location of the Pacific-Antarctic-Nazca triple junction, from the Valdivia FZ system to the Chile FZ (Figure 13).

Implications to General Models of Microplate Evolution

The evolution of the Friday microplate differs from that of other known extinct microplates. Based on microplates worldwide, *Mammerickx et al.* [1988] described the evolution of a microplate to involve (1) initial rifting, offset from another ridge, (2) an interval when both ridges are active, (3) gradual failure of one ridge, and (4) resumption of full spreading at the dominant ridge and preservation of a microplate (initially) near this ridge. While more detailed

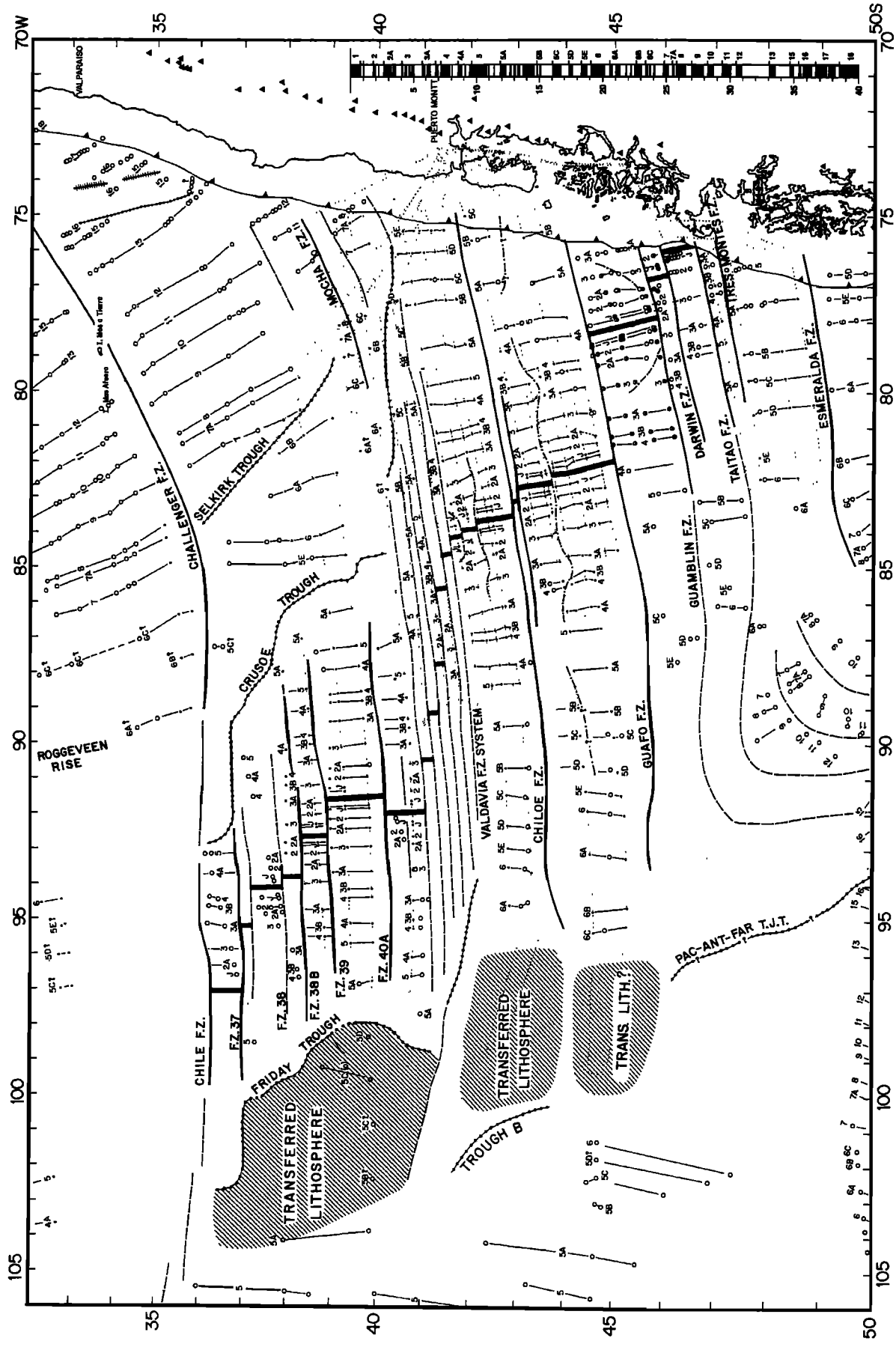

Figure 14. Tectonic interpretation of the Chile ridge. The 1990 LDEO-NRL aeromagnetic survey tracks are shown in light dotted lines. Solid magnetic anomaly points were determined from aeromagnetic data; half-filled magnetic anomaly points were determined from RRS *Charles Darwin* shipboard data; open circle magnetic anomaly points were determined from all other shipboard data. Triangles on land are active volcanoes compiled by the Smithsonian Institution.

models of microplate evolution have been developed [*Schouten et al.*, 1993, and references therein], these basic steps have remained. At the Friday microplate we see evidence for the first two steps described above, but neither ridge ever failed. Instead, after microplate extinction, both ridge axes of the microplate continued spreading and were "captured" as portions of major plate boundaries. This significant difference results in a process we call "stepwise" triple junction migration.

Effects of Ridge Subduction

The southern end of the Chile ridge is actively being subducted down the Chile trench. *Herron et al.* [1981] were the first to make the surprising observation that the actively subducting ridge axis has very little effect on the seafloor spreading process near the trench axis. This observation has been further supported by the observations on multichannel seismic, Sea Beam and GLORIA surveys [*Cande et al.*, 1988; *Cande et al.*, 1990; *Tebbens et al.*, 1990]. The new tectonic maps in this paper also reveal no evidence for Nazca plate breakup or Chile ridge rotation associated with ridge subduction. This differs from the subduction of the Pacific-Farallon ridge off North and Central Americas, where *Menard* [1978] found evidence for "pivoting subduction," where small portions separate from the main oceanic plate and rotate. *Herron et al.* [1981] suggested the lack of "pivoting subduction" at the Chile ridge is probably due to the geometry of plate interaction: (1) the angle between the spreading center on the Chile ridge and the Peru-Chile trench is only about 15° and perhaps too small to require pivoting; and (2) the offsets along the Chile ridge displace the ridge crest away from the trench in the opposite sense to the Farallon plate boundary in the northeast Pacific. In addition, "pivoting subduction" in the northeast Pacific is associated with the subduction of relatively young, uniform age Farallon crust. In contrast, while near zero-age Nazca crust is subducting at the colliding section of the Chile ridge, older Nazca plate crust (up to ~35 Myr old) is subducting farther north [*Cande and Haxby*, 1991]. Plate subduction appears to be the dominant driving force of plate motions with older, colder, denser subducting crust providing greater driving force [*Forsyth and Uyeda*, 1975; *Lithgow-Bertelloni and Richards*, 1995]. Subduction of the older sections of Nazca and Antarctic plates beneath South America may dominate Chile ridge plate motions, including the subducting ridge segment, and may help explain why "pivoting subduction" is not observed.

Conclusions

Data from a recent aeromagnetic survey have been combined with satellite altimetry data to construct a detailed tectonic map of the Chile ridge. The tectonic interpretation of this work is synthesized in Figure 14. The Chile ridge extends from the Juan Fernandez microplate to the Chile Margin triple junction and includes a total of 1380 km of ridge axis offset by 18 transform faults, including two complex fault systems (Table 1). Three nontransform offsets (and their off-axis traces) have also been identified.

Chile ridge spreading rates were determined for 17 intervals between 23 Ma and the Present (Table 2). Times of decreases in spreading rate were found to correlate with times of major Chile ridge-trench collisions.

The Valdivia FZ system is composed of six closely spaced (22-27 km offset) FZs separating short ridge segments which have been continuously active for the last 15 Myr. The Valdivia FZ system evolved from a single long left-lateral offset transform connecting the Chile ridge to the Pacific-Antarctic-Nazca triple junction at the time of a 10° counterclockwise rotation in spreading at chron 5C.

A plate boundary reorganization at chron 5A involved the northward propagation of a ridge axis from the Valdivia FZ system to the Chile FZ; two pseudofaults, the Crusoe and Friday troughs, were formed as a result. This event transferred lithosphere from the Nazca plate to the Antarctic plate to form the Friday microplate. The Friday microplate differs from previously studied extinct microplates in that both ridge axes of the microplate continued spreading; they were "captured" by major ridge axes. The east and west ridge axes of the extinct microplate are now segments of the Chile and Pacific-Antarctic ridges, respectively. The chron 5A reorganization, which included rift propagation, microplate formation, and microplate extinction with no failed ridge, resulted in a 500 km northward stepwise migration in the location of the Pacific-Antarctic-Nazca triple junction.

Acknowledgments. We thank the dedicated personnel of the Naval Research Laboratory Flight Detachment and Operational Services. The work was initiated as part of S.F.T.'s dissertation when S.F.T. and S.C.C. were both at Lamont-Doherty Earth Observatory of Columbia University. G. Westbrook provided magnetic and bathymetric data from RRS *Charles Darwin* cruise 36-88. D. Handschumacher provided Project Magnet aeromagnetic data collected by the Office of Naval Research program element ONR-61153N under the direction of H.C. Eppert Jr. W. Haxby provided Geosat data and assistance prior to the 1990 aeromagnetic survey. D. Sandwell provided access to computer programs and early access to the *Sandwell and Smith* [1992] gravity grid. This paper benefited from discussions with and/or reviews of T. Atwater, S. Carbotte, W. Haxby, K. Klitgord, P. Lonsdale, M. Kuykendall, D. Naar, M. Tivey, and, especially, H. Schouten who explained his microplate model [*Schouten et al.*, 1993] and its implications for the Friday microplate. B. Batchelder drafted Figures 4 and 5. This research was supported by National Science Foundation grant OCE-89-18612.

References

Anderson-Fontana, S., J. F. Engeln, P. Lundgen, R. L. Larson, and S. Stein, Tectonics and evolution of the Juan Fernandez microplate at the Pacific-Nazca-Antarctic triple junction, *J. Geophys. Res., 91*, 2005-2018, 1986.

Anderson-Fontana, S., J. F. Engeln, P. Lundgren, R. L. Larson, and S. Stein, Tectonics of the Nazca-Antarctic plate boundary, *Earth Planet. Sci. Lett., 86*, 46-56, 1987.

Batiza, R., Failed rifts, in *The Geology of North America*, Vol. N, *The Eastern Pacific Ocean and Hawaii*, vol. N, edited by E.L. Winterer et al., pp. 177-186, Geol. Soc. of Am., Boulder, Colo., 1989.

Bird, R. T., and D. F. Naar, Intratransform origins of mid-ocean microplates, *Geology, 22*, 987-990, 1994.

Cande, S. C., and W. F. Haxby, Eocene propagating rifts in the southwest Pacific and their conjugate features on the Nazca plate, *J. Geophys. Res., 96*, 19609-19622, 1991.

Cande, S. C., and D. V. Kent, A new geomagnetic polarity time scale for the Late Cretaceous and Cenozoic, *J. Geophys. Res., 97*, 13917-13951, 1992.

Cande, S. C., and D. V. Kent, Revised calibration of the geomagnetic polarity timescale for the Late Cretaceous and Cenozoic, *J. Geophys. Res., 100*, 6093-6095, 1995.

Cande, S. C., and R. B. Leslie, Late Cenozoic tectonics of the southern Chile trench, *J. Geophys. Res., 91*, 471-496, 1986.

Cande, S. C., R. B. Leslie, J. C. Parra, and M. Hobart, Interaction between the Chile ridge and Chile trench: Geophysical and geothermal evidence, *J. Geophys. Res., 92*, 495-520, 1987a.

Cande, S. C., P. R. Vogt, and P. J. Fox, Detailed investigation of a flowline corridor in the South Atlantic, II, A survey of 50 to 70 m.y. old crust on the west flank (abstract), *Eos Trans. AGU, 68,* 1491, 1987b.

Cande, S. C., S. D. Lewis, N. Bangs, S. F. Tebbens, and R. Forman, Interaction of the Chile ridge and Chile trench: Preliminary results from a Sea Beam and MCS survey, *Eos Trans. AGU, 69,* 1407, 1988.

Cande, S. C., J. L. LaBrecque, R. L. Larson, W. C. Pitman III, X. Golovchenko, and W. F. Haxby, Magnetic lineations of the world's ocean basins, *AAPG Map Ser.,* Am. Assoc. of Pet. Geol., Tulsa, Okla., 1989.

Cande, S. C., S. D. Lewis, N. Bangs, S. F. Tebbens, and G. K. Westbrook, The Chile ridge/Chile trench collision zone: A rift valley disappears beneath a continental margin, *Eos Trans AGU, 71,* 1565, 1990.

Cande, S. C., C. A. Raymond, J. Stock and, W. F. Haxby, Geophysics of the Pitman fracture zone and Pacific-Antarctic plate motions during the Cenozoic, *270,* 947-953, 1995.

Ewing, M., and B. C. Heezen, Some problems of Antarctic submarine geology, in *Antarctic in the International Geophysical Year, Geophys. Monogr. Ser.,* vol. 1, edited by A. Crary et al., pp. 75-81, AGU, Washington, D.C., 1956.

Forsyth, D., and S. Uyeda, On the relative importance of the driving forces of plate motion, *Geophys. J. R. Astron. Soc., 43,* 163-200, 1975.

Fox, P. J., and D. G. Gallo, The geology of North Atlantic transform plate boundaries and their aseismic extensions, in *The Geology of North America,* vol. M, The *Western North Atlantic Region,* edited by P.R. Vogt, pp. 157-172, Geol. Soc. of Am., Boulder, Colo., 1986.

Fox, P. J., and D. G. Gallo, Transforms of the eastern central Pacific, in *The Geology of North America,* vol. N, *The Eastern Pacific Ocean and Hawaii,* edited by E.L. Winterer et al., pp. 111-124, Geol. Soc. of Am., Boulder, Colo., 1989.

Handschumacher, D. W., Post-Eocene plate tectonics of the eastern Pacific, in *The Geophysics of the Pacific Ocean Basin and Its Margin, Geophys. Monogr. Ser.,* vol. 19, edited by G.H. Sutton et al., pp. 177-202, AGU, Washington, D.C., 1976.

Harland, W.B., R. Armstrong, A. Cox, L. Craig, *A. Smith, and D. Smith, A geologic Time Scale 1989,* 263 pp., Cambridge University Press, New York, 1990.

Herron, E. M., Crustal plates and sea-floor spreading in the southeastern Pacific, in *Antarctic Oceanology I, Antarct. Res. Ser.,* vol. 15, edited by J.L. Reid, pp. 229-237, AGU, Washington, D.C., 1971.

Herron, E. M., Sea-floor spreading and the Cenozoic history of the east-central Pacific, *Geol. Soc. Am. Bull., 83,* 1671-1692, 1972.

Herron, E. M., and D. E. Hayes, A geophysical study of the Chile Ridge, *Earth Planet. Sci. Lett., 6,* 77-83, 1969.

Herron, E. M., S. C. Cande, and B. R. Hall, An active spreading center collides with a subduction zone: A geophysical survey of the Chile margin triple junction, in *Nazca Plate: Crustal Formation and Andean Convergence,* edited by L.D. Kulm et al., Mem. Geol. Soc. of Am., *154,* 683-701, 1981.

Hey, R., A new class of "pseudofaults" and their bearing on plate tectonics: A propagating rift model, *Earth Planet. Sci. Lett., 37,* 321-325, 1977.

International Association of Geomagnetism and Aeronomy, Data Imaging Working Group (IAGA, DIWG), International geomagnetic reference field revision 1987, *IAGA News, 26,* 87-92, 1987.

Klitgord, K. D., S. P. Heustis, J. D. Mudie and R. L. Parker, An analysis of near-bottom magnetic anomalies: Sea-floor spreading and the magnetized layer, *Geophys. J. R. Astron. Soc., 43,* 387-424, 1975.

Klitgord, K. D., J. D. Mudie, P. A. Larson and J. A. Grow, Fast sea floor spreading on the Chile ridge, *Earth Planet. Sci. Lett., 20,* 93-99, 1973.

LaBrecque, J. L., South Atlantic Ocean and adjacent Antarctic continental margin, Reg. Atlas Ser., *Atlas 13,* 21 sheets, Ocean Drill. Program, Mar. Sci. Int., Woods Hole, Mass., 1986.

Larson, R. L., R. C. Searle, M. C. Kleinrock, H. Schouten, R. T. Bird, D. F. Naar, R. I. Rusby, E. E. Hooft and H. Lasthiotakis, Roller-bearing tectonic evolution of the Juan Fernandez microplate, *Nature, 356,* 571-576, 1992.

Leg 135 Scientific Party, Evolution of backarc basins: ODP Leg 135, Lau Basin, *Eos, Trans. AGU, 73,* 241, 243, 246, 1992.

Lithgow-Bertelloni, C., and M. A. Richards, Cenozoic plate driving forces, *Geophys. Res. Lett., 22,* 1317-1320, 1995.

Lonsdale, P., Geomorphology and structural segmentation of the crest of the southern (Pacific-Antarctic) East Pacific Rise, *J. Geophys. Res., 99,* 4683-4702, 1994.

Macdonald, K. C., D. S. Scheirer, and S. M. Carbotte, Mid-ocean ridges: Discontinuities, segments and giant cracks, *Science, 253,* 986-994, 1991.

Mammerickx, J., The Foundation seamounts: Tectonic setting of a newly discovered seamount chain in the South Pacific, *Earth Planet. Sci. Lett., 113,* 293-306, 1992.

Mammerickx, J., and D. Sandwell, Rifting of old oceanic lithosphere, *J. Geophys. Res., 91,* 1975-1988, 1986.

Mammerickx, J., and S. M. Smith, GEBCO map of the Pacific Ocean, sheet 5-11, Can. Hydrogr. Serv., Ottawa, Ont., 1980.

Mammerickx, J., D. F. Naar, and R. L. Tyce, The Mathematician paleoplate, *J. Geophys. Res., 93,* 3025-3040, 1988.

Mayes, C. L., L. A. Lawver, and D. T. Sandwell, Tectonic history and new isochron chart of the South Pacific, *J. Geophys. Res., 95,* 8543-8567, 1990.

Menard, H. W., Fragmentation of the Farallon plate by pivoting subduction, *J. Geol., 86,* 99-110, 1978.

Menard, H. W., T. E. Chase, and S. M. Smith, Galapagos Rise in the southeastern Pacific, *Deep Sea Res., 11,* 233, 1964.

Molnar, P., T. Atwater, J. Mammerickx, and S. Smith, Magnetic anomalies, bathymetry and the tectonic evolution of the South Pacific since the Late Cretaceous, *Geophys. J.R. Astron. Soc., 40,* 383-420, 1975.

Morgan, W., P. R. Vogt, and D. F. Falls, Magnetic anomalies and sea floor spreading on the Chile rise, *Nature,* 222, 137, 1969.

Müller, R. D., D. T. Sandwell, B. E. Tucholke, J. G. Sclater, and P. R. Shaw, Depth to basement and geoid expression of the Kane Fracture Zone: A comparison, *Mar. Geophys. Res., 13,* 105-129, 1990.

Munschy, M., J. Dyment, M. O. Boulanger, D. Boulanger, J. D. Tissot, R. Schlich and M. F. Coffin, Breakup and seafloor spreading between the Kerguelen Plateau-Labuan Basin and the Broken Ridge-Diamantina Zone, *Proc. Ocean Drill. Program Sci. Results, 120,* 931-944, 1992.

Naar, D. F., Microplates, in *Encyclopedia of Earth System Science,* vol. 3, pp. 231-237, Academic, San Diego, Calif., 1992.

Naar, D. F., and R. N. Hey, Tectonic evolution of the Easter microplate, *J. Geophys. Res., 96,* 7961-7993, 1991.

Parmentier, E. M., and W. F. Haxby, Thermal stresses in the oceanic lithosphere: Evidence from geoid anomalies at fracture zones, *J. Geophys. Res., 91,* 7193-7204, 1986.

Parsons, B., and J. G. Sclater, An analysis of the variation of ocean floor bathymetry and heat flow with age, *J. Geophys. Res., 82,* 803-827, 1977.

Sandwell, D. T., Thermomechanical evolution of oceanic fracture zones, *J. Geophys. Res., 89,* 11401-11413, 1984.

Sandwell, D., Global marine gravity grid and poster developed (abstract), *Eos Trans. AGU, 74,* 35, 1993.

Sandwell, D., and W. H. F. Smith, Global marine gravity from ERS-1, Geosat and Seasat reveals new tectonic fabric (abstract), *Eos Trans. AGU, 73* (43), Fall Meet. Suppl., 133, 1992.

Schouten, H., K. D. Klitgord, and D. G. Gallo, Edge-driven microplate kinematics, *J. Geophys. Res., 98,* 6689-6701, 1993.

Searle, R. C., R. T. Bird, R. I. Rusby, and D. F. Naar, The development of two oceanic microplates: Easter and Juan Fernandez microplates, East Pacific Rise, *J. Geol. Society London, 150,* 965-976, 1993.

Shaw, P., An investigation of small-offset fracture zone geoid waveforms, *Geophys. Res. Lett., 15,* 192-195, 1988.

Small, C., and D. T. Sandwell, An abrupt change in ridge axis gravity with spreading rate, *J. Geophys. Res., 94,* 17383-17392, 1989.

Smith, W. H. F., and D. T. Sandwell, Marine gravity field from declassified Geosat and ERS-1 altimetry (abstract), *Eos Trans. AGU, 76* (46), Fall Meet. Suppl., F156, 1995.

Tebbens, S. F., Tectonic evolution of the southeast Pacific from Oligocene to Present, Ph.D. thesis, Columbia Univ., New York, 1994.

Tebbens, S. F., and S. C. Cande, South Pacific tectonic evolution from early Oligocene to Present: Pacific-Antarctic-Nazca triple junction migrations, *J. Geophys. Res.,* this issue.

Tebbens, S. F., G. K. Westbrook, S. C. Cande, N. Bangs, and S. D. Lewis, Preliminary interpretation of combined GLORIA and SeaBeam imagery in the vicinity of the Chile margin triple junction (abstract), *Eos Trans. AGU, 70*(43), 1353, 1990.

Wessel, P., and W. F. Haxby, Thermal stresses, differential subsidence, and flexure at oceanic fracture zones, *J. Geophys. Res., 95,* 375-391, 1990.

Wessel, P., and W. H. F. Smith, Free software helps map and display data, *EOS Trans. AGU, 72*, 441, 1991.

S.C. Cande, Scripps Institution of Oceanography, MS 0215, La Jolla, CA 92093. (e-mail: cande@gauss.ucsd.edu)

L. Kovacs, Naval Research Laboratory, Washington, DC 20375-5350. (email: skip@hp8c.nrl.navy.mil)

J.L. LaBrecque, Lamont-Doherty Earth Observatory of Columbia University, Palisades, NY 10964.

J.C. Parra, GEODATOS, Santiago, Chile.

S.F. Tebbens, Department of Marine Sciences, University of South Florida, St. Petersburg Campus, 140 Seventh Avenue South, St. Petersburg, FL 33701-5016. (e-mail: tebbens@marine.usf.edu)

H. Vergara, Servicio Hidrografico y Oceanografico do la Armada, Valparaiso, Chile.

(Received December 5, 1994; revised June 24, 1996;
accepted August 20, 1996.)